(12) INTERNATIONAL APPLICATION PUBLISHED UNDER THE PATENT COOPERATION TREATY (PCT)

(19) World Intellectual Property Organization
International Bureau

(43) International Publication Date
31 July 2003 (31.07.2003)

PCT

(10) International Publication Number
WO 03/062847 A1

(51) International Patent Classification[7]: G01R 33/387

(21) International Application Number: PCT/GB03/00313

(22) International Filing Date: 27 January 2003 (27.01.2003)

(25) Filing Language: English

(26) Publication Language: English

(30) Priority Data:

0201700.2	25 January 2002 (25.01.2002)	GB
0224706.2	24 October 2002 (24.10.2002)	GB

(71) Applicant *(for all designated States except US)*: **MEDICAL RESEARCH COUNCIL** [GB/GB]; 20 Park Crescent, London W1B 1AL (GB).

(72) Inventors; and

(75) Inventors/Applicants *(for US only)*: **WILSON, James** [GB/GB]; Flat D6, Hatfield College, Durham DH1 3RQ (GB). **JEZZARD, Peter** [GB/GB]; FMRIB Centre, John Radcliffe Hospital, Headington, Oxford OX3 9DU (GB).

(74) Agent: **KEITH W NASH & CO**; 90-92 Regent Street, Cambridge CB2 1DP (GB).

(81) Designated States *(national)*: AE, AG, AL, AM, AT, AU, AZ, BA, BB, BG, BR, BY, BZ, CA, CH, CN, CO, CR, CU, CZ, DE, DK, DM, DZ, EC, EE, ES, FI, GB, GD, GE, GH, GM, HR, HU, ID, IL, IN, IS, JP, KE, KG, KP, KR, KZ, LC, LK, LR, LS, LT, LU, LV, MA, MD, MG, MK, MN, MW, MX, MZ, NO, NZ, OM, PH, PL, PT, RO, RU, SD, SE, SG, SK, SL, TJ, TM, TN, TR, TT, TZ, UA, UG, US, UZ, VN, YU, ZA, ZM, ZW.

(84) Designated States *(regional)*: ARIPO patent (GH, GM, KE, LS, MW, MZ, SD, SL, SZ, TZ, UG, ZM, ZW), Eurasian patent (AM, AZ, BY, KG, KZ, MD, RU, TJ, TM), European patent (AT, BE, BG, CH, CY, CZ, DE, DK, EE, ES, FI, FR, GB, GR, HU, IE, IT, LU, MC, NL, PT, SE, SI, SK, TR), OAPI patent (BF, BJ, CF, CG, CI, CM, GA, GN, GQ, GW, ML, MR, NE, SN, TD, TG).

Published:
— *with international search report*

For two-letter codes and other abbreviations, refer to the "Guidance Notes on Codes and Abbreviations" appearing at the beginning of each regular issue of the PCT Gazette.

(54) Title: OPTIMIZATION OF STATIC MAGNETIC FIELD HOMOGENEITY USING PASSIVE SHIMS

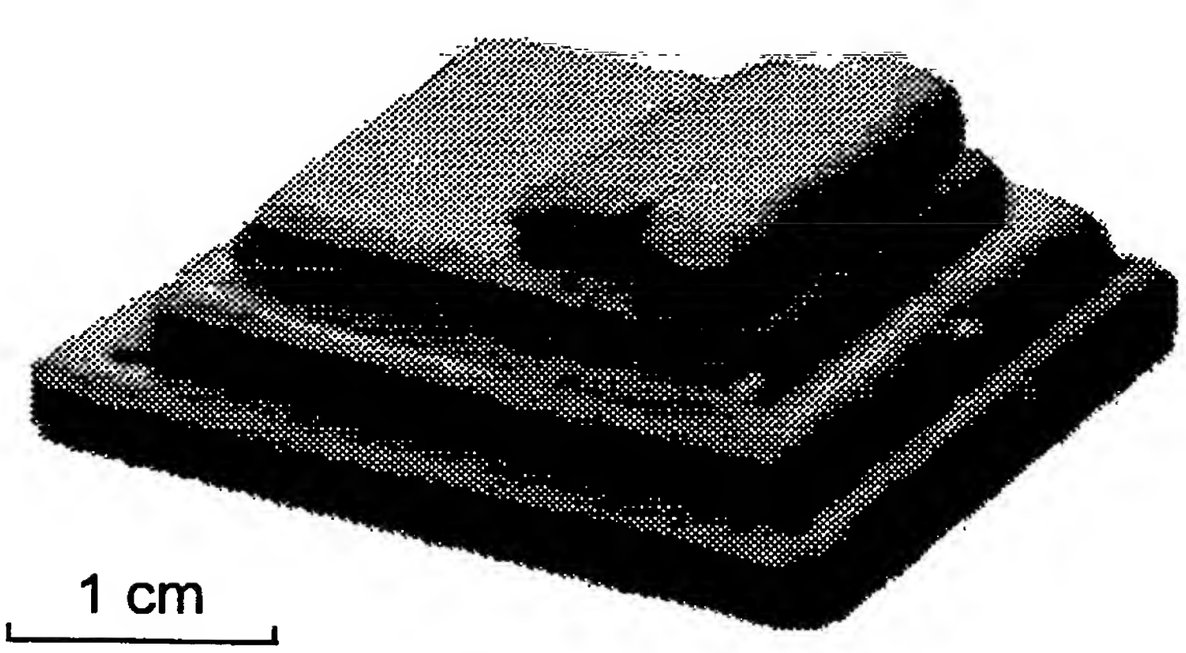

(57) Abstract: Disclosed is a method of obtaining magnetic resonance data regarding a sample, the method comprising the steps of: a) placing the sample within a suitable high flux density magnetic field, which field is substantially homogeneous prior to introduction of the sample; and wherein the presence of the sample causes local inhomogeneities in the magnetic field; and b) causing to be present, adjacent to the sample, a passive shim comprising sufficient amount of a highly diamagnetic substance as to reduce the inhomogeneity in the magnetic field caused by the sample.

WO 03/062847 A1

Title: OPTIMIZATION OF STATIC MEGNETIC FIELD HOMOGENEITY USING PASSIVE SHIMS.

Field of the Invention

The invention relates to a method of imaging samples, especially a human or animal body, and to apparatus for use in the method.

Background of the Invention

A considerable array of non-invasive imaging techniques are now available to study the interior of the human or animal body. Such techniques may be especially useful for clinical prognosis and/or diagnosis, assessing responses to various therapies, and also for research purposes.

Among such techniques is magnetic resonance imaging (MRI), which involves the production of images by exposing a subject to be examined to a strong, static magnetic field. By way of explanation certain nuclei, especially hydrogen nuclei, are subject to nuclear magnetic moments (i.e. spin) and when the nuclei are in a strong magnetic field the nuclear moments can only take up certain discrete orientations, each orientation corresponding to a different energy state. Transitions between these energy states can be induced by the application of radio frequency radiation. This phenomenon is referred to as nuclear magnetic resonance. The resonant frequency depends on the precise environment of the nucleus in question. This forms the basis of MRI, in which multiple projections are combined to form images of sections through a body or other sample. Linear gradients in the magnetic field enable spatial features to be distinguished. A more detailed explanation of the principles underlying MRI is provided in US 6,294,972.

MRI is particularly employed to study the brain, and in this respect functional MRI (fMRI) is a popular technique. In fMRI the operation of the brain is analysed during performance

of a particular task, and the resulting images are compared with those obtained when the subject is not performing the task in question. Typically the differences between the 'task' images and the control images are very small, and it is therefore necessary to obtain a large number of images in order for statistically significant conclusions to be drawn.

In order to perform any sort of MRI technique it is generally desirable to ensure that the applied static magnetic field (referred to as the B0 field) is as homogeneous as possible. To increase the homogeneity of the B0 field it is well known to practice "shimming". Such shimming may be "active" or "passive". Active shimming involves the use of secondary "shim" coils which correct, for example, minor deviations in the B0 field generated by imperfections in the magnet windings of the primary coils. Passive shimming involves the positioning of shims (generally ferromagnetic materials, such as soft iron) in or around the magnets to influence the resulting magnetic field.

Whilst shimming of this sort can establish an almost perfectly homogeneous B0 field in the bore of the MRI scanner, unfortunately the introduction of the subject into the scanner can itself create local inhomogeneities, in particular close to tissue/air and tissue/bone interfaces. This problem is well-known to those in the field (see, for example, Jezzard & Clare, 1999 Hum. Brain Mapping 8, 80-85, and Howseman *et al*, 1999 Phil. Trans. R. Soc. Lond. B 354, 1179-1194). This problem is especially pronounced in fMRI where very high B0 flux densities (2 Tesla or more) and rapid data acquisition are involved. These inhomogeneities cause "susceptibility artifacts" in the resulting images. Susceptibility artifacts are of two types: (a) loss of signal, and (b) geometric distortion. Susceptibility artifacts are especially pronounced in the human inferior frontal cortex (IFC). This is unfortunate as the IFC is a region of the brain of considerable interest to researchers, being known to participate in the processing of olfaction, taste, emotion and memory, and has been implicated in disorders such as schizophrenia, depression, anxiety, attention deficit hyperactivity disorder and drug abuse. Merboldt *et al* (2001 Neuroimage 14, 253-257) have considered what they call "The Susceptibility Problem" in the context of fMRI analysis of the human amygdala. They concluded that "functional mapping of the amygdala by BOLD (blood oxygenation-level dependent) MRI techniques requires high

spatial resolution along all three dimensions.... The only real alternative....may evolve from the use of flow-based functional mapping techniques".

Others have tried to address the problem by using local ferromagnetic shims (e.g. Jesmanowicz *et al*, 2000 Proc. 8th ISMRM, 1378 and US 6,294,972) but the solution is not very useful since it is of limited effectiveness, takes a long time to implement and requires the careful positioning of passive ferroshim inserts attached to a local head coil.

The present inventors have found a simple and practical method of ameliorating susceptibility artifacts which is applicable to any method of magnetic resonance imaging but especially those which require the use of high magnetic flux densities (1.5T or higher). The invention involves the use of a passive shim comprising a highly diamagnetic material.

By way of explanation, when a substance is introduced into a vacuum in a region where there is an existing magnetic field with a flux density of B0, the flux density is altered to a new value, B. The value of B depends on the relative permeability μr of the substance ($\mu r = B/B0$). The magnetic susceptibility, χ, of the substance is defined as $\chi = \mu r - 1$.

In essence all materials may be classified as falling into one of three groups: ferromagnetic; paramagnetic and diamagnetic.

A few materials are ferromagnetic. They are strongly affected by magnetic fields and have very high μr values (typically 10^4). Ferromagnetic elements include iron, nickel and cobalt, and a number of oxides and alloys of these elements are also ferromagnetic.

However, the great majority of materials are paramagnetic or diamagnetic. In paramagnetic materials an applied magnetic field tends to align the magnetic moments of the atoms or molecules and the material acquires temporary magnetization in the direction of the field: the magnetization is lost when the applied magnetic field is removed. Paramagnetic materials have a positive magnetic susceptibility. In diamagnetic materials the converse applies. That is, the magnetic susceptibility is negative and the induced magnetization opposes the magnetizing field. Moreover, such paramagnetism or diamagnetism is usually extremely

weak: paramagnetic materials typically have a relative permeability very slightly greater than 1 (e.g. 1.001), whilst diamagnetic materials typically have a relative permeability very slightly less than 1 (e.g. 0.99999). Typically diamagnetic materials have a very small negative susceptibility of about 10^{-5} (e.g. human tissue or water typically has a susceptibility of about –9ppm).

Nevertheless, there are some materials, including bismuth and graphite, which are quite strongly diamagnetic, with a relative permeability of the order of 0.9999 and hence a magnetic susceptibility of –100ppm or so.

Summary of the Invention

In a first aspect the invention provides a method of obtaining magnetic resonance data regarding a sample, the method comprising the steps of:

a) placing the sample within a suitable high flux density magnetic field, which field is substantially homogeneous prior to introduction of the sample; and wherein the presence of the sample causes local inhomogeneities in the magnetic field; and

b) causing to be present, adjacent to the sample, a passive shim comprising sufficient amount of a highly diamagnetic substance as to reduce the inhomogeneity in the magnetic field caused by the sample.

The properties of a magnetic field suitable for producing magnetic resonance data will be apparent to those skilled in the art. For present purposes a high flux density is understood to refer to a magnetic field having a flux density of at least 1 Tesla (1T), preferably at least 1.5T. The method of the invention is especially useful in the performance of magnetic resonance imaging (MRI), particularly fMRI which generally requires the use of magnetic fields with very high flux densities (which, for present purposes, may be defined as at least 2T, preferably 3T or more).

A magnetic field may be considered as substantially homogeneous, for the purposes of the present specification, if the flux density of the field over the region of the sample from which

data is being acquired varies by less than 0.5ppm, preferably by less than 0.2ppm and most preferably by less than 0.1ppm.

The sample may be an inert material or, more typically, may be a human or animal body. The highly diamagnetic material comprised within the passive shim may be, for example, bismuth or graphite. Due to the relatively high toxicity of bismuth, graphite is generally preferred. In particular, certain forms of graphite are found to be especially diamagnetic, such as pyrolytic graphite. Preferred examples of pyrolytic graphite include "highly ordered pyrolytic graphite" (HOPG) and "constantly nucleated pyrolytic graphite" (CNPG). Suitable pyrolytic graphite is commercially available, for example, from Minerals Technologies Inc. (NY 10174, USA), or its subsidiary Minteq International, Inc. (PA, USA). By way of explanation, graphite exists in many forms having differing amounts of impurities. This leads to a large range of values for its magnetic susceptibility. Pyrolytic graphite, manufactured by chemical vapour deposition, has a high degree of preferred crystallographic orientation of the *c*-axes perpendicular to the surface substrate. Constantly nucleated Pyrolytic Graphite (CNPG), typically produced by stress annealing at high temperatures, possesses an angular spread of the *c*-axes of the crystallites of less than 1° resulting in a highly anisotropic magnetic susceptibility. Perpendicular to the graphite basal plane, CNPG is the most diamagnetic solid substance known.

For present purposes, a highly diamagnetic substance may be defined as any substance having a magnetic susceptibility of –200ppm or less (i.e. a more negative value), preferably –300ppm or less, more preferably –400ppm or less, and most preferably –450ppm or less. It is believed that the theoretical maximum magnitude of diamagnetic susceptibility is about –600ppm, but it may be that this theoretical maximum value is impossible to ever obtain in practice.

What constitutes a sufficient amount of the highly diamagnetic substance will depend on the magnitude of the diamagnetism of the material in question. The person skilled in the art can readily conduct non-inventive trial-and-error experimentation in order to ascertain a sufficient amount of material in the passive shim for use in the invention. For example, using pyrolytic graphite with a magnetic susceptibility of the order of –450ppm, the

inventors find that a mass of about (12) gm of pyrolytic graphite for a mouth shim gave satisfactory results.

The magnetic resonance data obtained by the method are conveniently used to produce magnetic resonance images of the sample. The sample is generally an animal, or more preferably, a human subject. Any part of the animal or human body may be imaged, but the method of the invention is especially useful for imaging of the neck and/or head region, and especially for imaging of part or all of the brain.

Imaging techniques which may benefit from the method of the invention include, but are by no means limited to: localised spectroscopy and spectroscopic imaging, MRI, and especially fMRI techniques, such as Perfusion contrast fMRI and BOLD (Blood Oxygenation-level Dependent) fMRI methods such as Echo Planar Imaging (EPI, Merboldt *et al*, 2000 J. Magn. Reson. 145, 184-191), Spiral Imaging (Noll *et al*, 1995 J. Magn. Reson. Imaging 5), Fast Low Angle Shot (FLASH) Imaging, also known as Spoiled Grass (SPGR) imaging (Haase *et al*, 1986 J. Magn. Reson. 67, 212-222) and Principles of Echo-shifting with a Train of Observations (PRESTO Liu *et al*, 1993 Magn. Reson. Med. 30, 764).

Typically the local inhomogeneities in the magnetic field caused by the sample, and corrected by the method of the invention, are due to magnetic susceptibility differences in the sample. Typical examples include those caused by tissue/air and tissue/bone interfaces. In particular, when imaging the brain, susceptibility artifacts may be caused by one or more of the following: ethmoid, sphenoid or frontal sinuses, the mastoid air cells, and the external auditory canal.

Depending on the number and nature of the field inhomogeneities it is desired to correct, it may be advantageous to use a plurality of passive shims, at least one of which, and possibly more, will comprise a highly diamagnetic substance. In some embodiments it may be desirable to use one or a plurality of highly diamagnetic passive shims, with or without one or more ferromagnetic or (more preferably) paramagnetic passive shims, located so as to optimise the homogeneity of the B0 field in the region of the sample under investigation.

More especially, the term 'adjacent' as used herein is to be understood as encompassing those situations in which the highly diamagnetic shim is positioned within a cavity of the subject, especially where the subject is a human or animal body. Further, it should be noted that the term "adjacent" does not necessarily require that the passive shim is in direct physical contact with some part of the sample or subject, although this is preferred. It will generally be sufficient for the highly diamagnetic shim to be positioned within 5cm of contacting the subject, more preferably within 3cm of contacting the subject, and most preferably within 1cm of contacting the subject.

In particular, the inventors have found that positioning of a highly diamagnetic passive shim within the mouth of a subject can greatly reduce the magnetic field inhomogeneities (believed to be caused primarily by the ethmoid and sphenoid sinuses) affecting imaging of the inferior frontal cortex of the brain, which is responsible for many executive brain functions and whose malfunction is known to be involved in depression and schizophrenia.

The inventors have also found that insertion of a highly diamagnetic passive shim into the ear canal can reduce the magnetic field inhomogeneities which affect imaging of the inferior temporal lobe, which are believed to be caused, at least in part, by the mastoid air cells (predominantly) and (to a lesser extent) the external auditory canal.

The mastoid air cells responsible, at least in part, for the inhomogeneity affecting imaging of the inferior temporal cortex, are positioned posterior to the ear. Accordingly it may not be possible to remove the inhomogeneity solely by positioning a highly diamagnetic material within the ear canal, without creating an inhomogeneity elsewhere. In order to address this problem it may be advantageous to position a highly diamagnetic passive shim behind the ear, which is closer to the mastoid air cells. One way of achieving this might be to use a "hearing aid" type arrangement, with a locating/retaining means engaging with the ear lobe and/or ear canal, and the highly diamagnetic material be attached to the locating/retaining means and nestling behind the ear lobe.

The optimum size, shape and positioning of the passive shim will depend primarily on the size, shape and position of the B0 field inhomogeneity that the shim is intended to correct.

Simple trial and error can be employed to determine the optimum characteristics in any particular case. This may be by physical performance of trials and inspection of the resulting images and/or by computer simulation.

The inventors have found empirically or by computer-modelled simulation that the inhomogeneity affecting the inferior frontal region can be ameliorated by locating a highly diamagnetic shim at any one of the following positions: under the chin, between the teeth, or (most preferably) adjacent the roof of the mouth. Similarly the inhomogeneity affecting the anterior frontal region can be reduced by locating a highly diamagnetic shim upon or just beneath the brow. Finally a highly diamagnetic shim located in the ear canal, or on, below or behind the ear lobe can reduce the inhomogeneity affecting the inferior temporal region.

Clearly, where a shim is intended to be inserted into the ear canal at least that portion of the shim which enters the canal must be suitably dimensioned, so as to avoid discomfort to the subject. Equally, if the shim is to be positioned within the mouth, suitable dimensions are necessary in respect at least of that portion which enters the mouth.

The position of the passive shim within the mouth can affect the quality of the images obtained of the frontal lobe. Desirable locations include (a) between the teeth, more especially between the molars or pre-molars, with highly diamagnetic material on each side of the mouth; and/or (b) on or near the roof of the mouth. In general, particularly in position (b), the further towards the rear of the mouth, the better the quality of the data obtained regarding the frontal lobe of the brain, but the shim cannot be positioned so far to the rear of the mouth that the subject is likely to choke. Ergonomic shaping of the shim can be employed to minimise any discomfort to the subject, especially where the shim is intended to contact or engage with the subject's body, or to be located within a body cavity.

In order to assist with positioning of the one or more shims, it may be advantageous to provide the shim with some sort of positioning guide. This could take the form of a frame strapped to the subject's body, or a cap attached to the subject's head. A 'headphone' or 'earplug' type arrangement could be used to position and retain one or more passive shims on, in or around the ear or ears of a subject. In relation to shims to be positioned in the

mouth, these could be provided, for example, as part of a 'gumshield' type arrangement or incorporated into a 'bite bar' held between the subject's teeth.

In particular, the inventors have found that subjects are at ease when retaining the mouth shim within their mouths for a period of approximately 25 minutes. After the initial placement of a shim within the mouth, the rate of salivation increased, potentially leading to a significant increase in head motion. Allowing a subject to become more accustomed to the mouth shim before entering the scanner is expected to reduce salivation and subsequent head motion during the fMRI task close to normal levels. If necessary, integration of a mouth shim within a bite bar arrangement dramatically diminishes the presence of head motion over a period of up to 50 minutes. Head motion may also be limited by use of foam padding or, more effectively, by the use of a head restraint system. (D'Arcy *et al*, 2002 Proc. Intl. Soc. Magn. Res. Med. 10, 1408).

In some embodiments, the highly diamagnetic material may be highly anisotropic with respect to its magnetic susceptibility. Thus, for example, where the shim is of a relatively thin layer of material generally parallel to the roof of the mouth, the highly diamagnetic property may exist in the direction perpendicular to the roof of the mouth, but the material is not highly diamagnetic in the orthogonal direction.

In a particular embodiment, the invention provides a method of determining the presence or absence of a pathological condition affecting a human or animal subject, the method comprising the steps of:

(a) placing the subject within a suitable high flux density magnetic field, which field is substantially homogeneous prior to introduction of the subject, and wherein the presence of the subject causes local inhomogeneities in the magnetic field;

(b) causing to be present, adjacent to the subject, a passive shim comprising sufficient amount of a highly diamagnetic substance as to reduce the inhomogeneity in the magnetic field caused by the subject;

(c) obtaining magnetic resonance data from the subject and forming images of the interior of the subject using the data so obtained; and

(d) analysing the images to diagnose the presence or absence of the pathological condition.

The term 'diagnose' as employed herein is intended to be construed broadly, as encompassing the acquisition of any sort of information about a pathological condition (e.g. presence or absence, severity, extent, location, type or identity, and so on). The method can also be used to obtain information regarding the function of a normal brain or part thereof in healthy subjects (e.g. when performing a particular task).

In a second aspect the invention provides a passive shim for use in a magnetic resonance imaging technique, the passive shim comprising sufficient amounts of a highly diamagnetic substance (as herein defined) and being so dimensioned as to be locatable adjacent to a sample to be imaged, preferably adjacent to a human or animal body.

In one embodiment the shim further comprises a thin layer of material provided as a disposable covering, so that the shim may be used with a plurality of different subjects, the disposable covering being removed and replaced with a fresh covering after each use. In the same or another embodiment, the passive shim is so dimensioned as to be locatable in a body cavity of a human or animal subject. Preferably the body cavity is the mouth or the ear canal. Preferably the shim is shaped and sized so as to be locatable within the mouth cavity, adjacent to the roof of the mouth.

In a third aspect the invention provides a passive shim positioning device, the positioning device comprising a passive shim of highly diamagnetic material, and means for positioning (and preferably retaining) the passive shim in a particular location relative to the subject. In particular preferred embodiments the passive shim positioning device takes the form of one or more of the following: a gum shield, a bite bar, a headphone, an ear plug or ear plugs, or a frame for engagement with or attachment to a subject's head. It will be noted that these embodiments are not mutually exclusive and it may be advantageous, for example, to combine headphones or a head frame with an integral bite bar or gum shield, to position

simultaneously a plurality of passive shims, at least one of which will comprise a highly diamagnetic material. The one or more further shims may be ferromagnetic (if securely fastened to a base which will resist the magnetic force generated by the applied magnet field), or, more preferably, paramagnetic or diamagnetic to a greater or lesser extent. Generally highly diamagnetic or paramagnetic materials are desirable for the one or more further shims.

The shim positioning device is generally, but not necessarily, intended to locate shims so as to improve imaging of the subject's neck and/or head, more especially the subject's brain, and even more especially the inferior frontal cortex (IFC) region of the brain.

A shim in accordance with the present invention may be used in combination with any one or more compatible conventional methods described for susceptibility artifact reduction including, for example, those described by Ojemann *et al*, (1997 NeuroImage 6, 156-167); Merboldt *et al*, (2000 J. Magn. Reson. 145, 184-191); Gu *et al*, (2002 NeuroImage 17, 1358-1364); Stenger *et al*, (2002 Magn. Reson. Med. 78, 157-165); Blamire *et al*, 1996 Magn. Reson. Med. 36, 159-165); Deichmann *et al*, (2002 NeuroImage 15, 120-135); and Heberlein & Hu (2001, Proc. Intl. Soc. Magn. Res. Med. 9, 1157).

The various features of the invention will now be described by way of illustrative example and with reference to the accompanying drawings, in which:

Figures 1-7 illustrate various numbers of image sections. Figures 1 and 3 comprise images of 25 sections of the B0 map of a human brain in the axial plane with (Figure 3) or without (Figure 1) a passive shim of highly diamagnetic material. Figures 2 and 4-7 show MRI sections of the human brain in the axial plane with (Figs. 4 and 7) or without (Figs. 2, 5 and 6) a highly diamagnetic passive shim;

Figures 8-10 comprise a series of images (in the axial, coronal and sagittal planes respectively) showing approximately desirable locations for shims containing highly diamagnetic material;

Figure 11 shows a shim positioning device, constructed for experimental purposes, in accordance with the invention;

Figure 12 shows a series of image sections obtained using a "structural" MRI technique;

Figure 13 shows a photograph of a mouth shim as used in Example 3 below, in accordance with the invention;

Figure 14 is a bar chart showing reduction in signal loss obtained using the mouth shim shown in Figure 13, for six different subjects A-F;

Figures 15 and 16 show a series of EPI images obtained in the presence or absence of a highly diamagnetic passive shim in accordance with the invention, as described in the text;

Figures 17(a)(b) show two views of the simulated B_0 field due to the mouth shim depicted in Figure 13;

Figure 18 shows a number of simulated B_0 maps for subject E in the presence or absence of a mouth shim in accordance with the invention, as described in the text;

Figures 19a and b show, respectively, midline sagittal views of the MR structural image and susceptibility map used in some experiments performed by the inventors (described in Example 5);

Figures 20a-f show a number of B_o difference maps for sagittal (left hand column), coronal (middle column) or axial (right hand column) sections obtained from B_o simulations with (panels b, d and f) or without (panels a, c and e) a mouth shim in accordance with the invention;

Figures 21a and 21b are graphs showing $<|\Delta B^j_{o,\theta}|>$ per ppm per degree for different angles of rotation for the IFC region (21a) or the whole brain (21b) with a shim (filled symbols) or

without a shim (empty symbols) in accordance with the invention, for rotation of the head about R_x (squares) or R_y (triangles);

Figures 21c and 21d are graphs showing the variation of $<|\Gamma j_\theta|>$ (in ppm per degree) with angle of rotation within the IFC (21c) or whole brain (21d) with a shim (filled symbols) or without a shim (empty symbols) in accordance with the invention, for rotation of the head about R_x (squares) R_y (triangles) or R_z (lozenges);

Figures 22a-f show a number of images of sagittal (left hand column), coronal (middle column) and axial (right hand column) views obtained in different ways with (22b, d and f) or without (22a, c and e) the assistance of a mouth shim in accordance with the invention;

Figures 23a-d are graphs showing variation of $<|G_z|>$ (a, b) or <|signal change|> (c,d) with angle of rotation within IFC (a, c) or brain (b, d) in the presence (filled symbols) or absence (empty symbols) of a shim in accordance with the invention; and

Figures 24a-f show a series of images obtained by various means by the inventors during an investigation of the effects of a shim in accordance with the invention on BOLD fmri experiments in a subject experiencing hypercapnia.

For the avoidance of doubt, the content of all documents mentioned in this specification are incorporated herein by reference.

Examples

Example 1

The inventors conceived of the idea of using a highly diamagnetic material as a passive shim in magnetic resonance imaging.

Figure 1 shows a typical B0 map of the human brain. The Figure comprises 25 sections in the axial plane. A perfectly homogeneous B0 field would be represented as a uniform

density gray across the whole brain. It is apparent however from the Figure (see especially Section Nos. 8-16) that inhomogeneities exist, and these might be expected to cause problems in data acquisition from the corresponding areas of the brain. This is indeed the result and this problem is well known to those skilled in the art.

Figure 2 shows a corresponding series of 25 actual Gradient Echo- Echo Planar Images (GE-EPI) obtained from a human brain in the axial plane.

In Figure 1 inhomogeneities are apparent (see Sections 8-12) in the inferior temporal cortex ("ITC") superior to the external auditory canal/mastoid air cells. These inhomogeneities cause corresponding loss of signal and geometric distortion (see dark areas in corresponding Sections 8-11 of Figure 2).

Equally, in Figure 1 inhomogeneities are apparent (see Sections 9-14) in the inferior frontal cortex ("IFC") superior to the sphenoid and ethmoid sinuses. These cause loss of signal and geometric image distortion (see Sections 11-15) in Figure 2. Also in Figure 1, inhomogeneities in the anterior frontal cortex (Sections 12-15) superior to the frontal sinus cause minor signal loss in addition to the substantial geometric distortion (see Sections 14-17) apparent in Figure 2.

In an attempt to reduce the inhomogeneity in the inferior frontal cortex, the inventors made a highly diamagnetic passive shim for location in the mouth of a subject. The shim comprised pyrolytic graphite (PG, obtained from Minteq International Inc. PA). The magnetic susceptibility of PG is anisotropic, varying from –450ppm (PG plane perpendicular ($\perp$) to B0) to –85ppm (PG plane parallel ($\parallel$) to B0) (Simon *et al*, 2001 Am. J. Phys. 69, 702-713.) Small variations in the diamagnetic susceptibility may be expected in pyrolytic graphite from different sources.

The "mouth shim" was constructed from two sheets of PG (each sheet 3 x 23 x 40mm, PG plane within sheet), covered in thin plastic, and placed flat against the roof of the subject's mouth. It was safely held in place by a mouthpiece and supported by the subject's tongue for these preliminary studies. An experimental device is shown in Figure 11 (with a ruler for

scale shown in the background). Commercial shim devices in accordance with the invention will be ergonomically shaped for user comfort and convenience. Axial B0 maps and GE EPIs were obtained, following an active global brain shim (Wilson & Jezzard 2001 Proc. 9th ISMRM:1230), without and with the mouth shim – no other parameters were altered.

Results

All data were acquired using a 3T Varian Inova spectrometer.

For all sequences: data matrix = 64 x 64, 25 slices and voxel size = 4 x 4 x 6 mm. For the symmetric - asymmetric spin echo B0 map: TR/ TE/ asymmetry time = 1250/20/2.5 ms. For the EPI: TR/TE = 3000/30 ms, readout bandwidth = 100 kHz.

The distortion of B0 due to the mouth shim was simulated by solving Maxwell's equations using a perturbation method. The experimental mouth shim placement was located using a structural image. The associated simulated B0 was added to the B0 map obtained with no mouth shim to give the simulated B0 map with the mouth shim - this simple addition of B0 was found to be valid to first order.

Figure 3 shows a typical B0 map of the brain obtained when the subject is provided with the mouth shim. It is apparent (see Sections e.g. 9-14), by comparison with Figure 1 (which has the same grey level scaling applied), that the inhomogeneity in the IFC is greatly reduced, although the mouth shim does little, if anything, to reduce the inhomogeneity in the ITC. The anterior frontal inhomogeneity is also somewhat reduced.

Figure 4 is a series of six sections (corresponding to Section numbers 9-14 of the earlier figures) showing Gradient echo EPI images obtained when the subject is provided with the mouth shim. These may be directly compared with the images shown in Figure 5, which are for the same sections of the same subject in identical conditions, except that the mouth shim was removed. The improvement in reduction of signal loss and geometric distortion in the IFC is dramatic and readily apparent by comparison of Figures 4 and 5. Figures 4 and 5 may themselves be compared with Figure 12. Figure 12 shows a series of

"structural" MRI sections (using a sequence which is slower and less prone to susceptibility artifacts).

Computer analysis of the images revealed that, in relation to the IFC, the mean B0 offset and standard deviation were reduced by 70% and 28% respectively by the use of the mouth shim without, importantly, degrading the B0 field elsewhere. A computer-modelled simulation of the B0 map (with shim) was in extremely close agreement with the empirically-obtained B0 map: the mean difference over the whole brain was 0.04$\pm$ 0.06 ppm. The number of voxels in the IFC experiencing more than 75% signal loss (after image distortion correction) decreased by 74% using the mouth shim.

Example 2

Following the successful trial of the mouth shim, the inventors devised a PG earplug (12 x 10 x 5mm, PG plane $\perp$ to B0). Data were acquired as previously.

The GE-EPI images obtained without the earplug shim are illustrated in Figure 6, which shows section numbers 6-11. Taking the top of the Figure as "12 o'clock", the susceptibility artifacts in the ITC are apparent at approximately the 4 o'clock and 8 o'clock positions. Figure 7 shows the same section numbers, under identical conditions, except with a PG earplug type shim located in the left ear of the subject. A significant improvement in image quality is apparent, especially in the left ITC Sections 6-9.

When the images were analysed by computer it was found that the mean B0 offset and the standard deviation for the left ITC region were reduced by 74% and 8% respectively. The number of voxels in the left ITC experiencing more than 75% signal loss was reduced by 36%. Again, these improvements were obtained without degrading the B0 field or image quality at other parts of the brain.

Example 3

At least 7 different locations for a highly diamagnetic passive shim have been identified by the inventors as being of potential benefit in improving image quality:

position 1 – under chin

position 2 - under ear lobe (left and/or right)

position 3 – on the surface of the ear lobe, typically just posterior to the ear canal (left and/or

right)

position 4 - in ear canal (left and/or right)

position 5 – between teeth (left and/or right)

position 6 – on roof of mouth

position 7 – under brow (e.g. attached to prism glasses)

A highly diamagnetic passive shim at any one or more of positions 1, 5 and 6 has been demonstrated (experimentally or by computer simulation) to be of benefit in reducing the inferior frontal inhomogeneity. A highly diamagnetic shim at any one or more of positions 2, 3 or 4 has been shown experimentally to be of benefit in reducing the inhomogeneity in the inferior temporal region. A highly diamagnetic shim at position 7 has been shown (experimentally) to be of benefit in reducing the inhomogeneity affecting the anterior frontal region.

Figures 8-10 show a series of sections, in the axial, coronal and sagittal planes respectively, on which the approximate location of positions 1-7 is indicated. The reference numerals refer to the position number. The white rectangular areas indicate the approximate size and location of the shims used by the inventors.

Example 4

Having demonstrated the feasibility of improving the homogeneity of the B_0 field using the mouth shim in one subject (Example 1) the inventors extended their investigations by conducting trials of an improved mouth shim with additional subjects.

The improved mouth shim was constructed from 4 plates of CNPG, as shown in Figure 13, and shaped to fit within the roof of the mouth with ease, the plates being perpendicular

to B_0. The total volume of CNPG is 6.1 cm^3. The CNPG is fully enclosed within a customised mouth mould of the subject made from polymorph plastic (Middlesex Teaching Resources, UK) providing a good fit within the roof of the subject's mouth. The lower section of the rigid mouth mould extends laterally from the mouth shim and fits securely between the subject's teeth. The anterior section of the mouth mould extends out of the mouth and prevents accidental descent of the mouth shim further into the mouth. Use of the disposable polymorph material allows re-use of the CNPG material. The improved mouth shim is illustrated in Figure 13.

A preliminary "ear shim" was also constructed to improve B_0 homogeneity in the ITCs. It was constructed from 6 rectangular plates of HOPG each measuring 19×10 mm, forming a cuboid of volume 3.4 cm^3.

Experiment

All experiments were performed on a 3 T Varian Inova spectrometer fitted with a Magnex SGRAD head gradient coil. Room-temperature shim coils of first and second order were used along with a quadrature birdcage head coil.

Six volunteers (4 male, 2 female), termed subjects A though F, having given informed consent, were scanned in compliance with local ethical committee requirements. The subject group was chosen to represent the distribution of IFC B_0 inhomogeneity size (defined as the volume of the IFC mask, described below) within the normal population as characterised by a sample of 15 volunteers. Neither the difference in the variance nor in the mean between our group of subjects and the population sample was found to be significant (variance ratio test: $p = 0.63$, $df = 5, 14$; independent two-sample t-test: $p = 0.736$, $df = 19$). The inventors therefore concluded that the range of IFC B_0 inhomogeneity sizes within the subject group reasonably represented the range of values within the larger population. The size of IFC B_0 inhomogeneity increased from subject A through to subject F.

B_0 mapping was performed with an axial symmetric and asymmetric multi-slice spin echo

acquisition with parameters: data matrix=64×64, 25 slices; slice thickness=6 mm; field of view (FOV)=256×256 mm; TR/TE/asymmetry time=1250/20/2.5 ms. To demonstrate the reduction in susceptibility artifact, an axial gradient-echo EPI sequence typical of an fMRI experiment at 3T was used. Spatial parameters were identical to the B_0 map; other parameters included: TR/TE=3000/30 ms and readout bandwidth=100 kHz. These parameters are typical for a BOLD fMRI study.

Without the mouth shim in place, a global shim of brain B_0 was performed, using the room-temperature shims, followed by acquisition of an EPI and B_0 map. The subject then placed the mouth shim in position without the subject being removed from the magnet. A global shim of brain B_0 was again performed and an EPI and B_0 map once more acquired. For three subjects, imaging with the mouth shim was performed prior to imaging without the mouth shim.

In addition to the above acquisitions, for subject C only, the effect of the ear shim was evaluated. An ear shim was placed inferior and posterior to but just touching each ear, lateral to the location of the subject's mastoid air cells. It was supported against the head and the ear using tape, the HOPG plates being perpendicular to B_0. A global shim of brain B_0 was subsequently run and a further EPI and B_0 map obtained.

Any remaining EPI geometric distortion was unwarped (Jezzard & Balaban 1995 Magn. Reson. Med. 34, 65-73) in-plane utilising the B_0 map (regularisation was applied to the B_0 map in the form of 2D Gaussian smoothing) (Jenkinson 2001 Neuroimage 13, 5165). For each subject, a manually defined brain mask was constructed using the magnitude-reconstructed spin-echo image acquired as part of the B_0 map in order to facilitate a whole-brain measure of B_0 improvement. In addition, an IFC mask was created for each subject to analyse the B_0 and EPI data within regions experiencing the most severe susceptibility artifact due to the presence of the ethmoid and sphenoid sinuses.

The purpose of the IFC mask was to estimate the number of voxels within the designated area that experience a signal loss of greater than 25%. In order to achieve this it is

necessary to compare the experimental data with an estimate of the image that would be obtained if there were no susceptibility artifacts present. This was accomplished by constructing an "ideal" tissue segmented image, derived from the subject's T_1-weighted structural scan, and corrected for the RF field (B_1) inhomogeneity of the RF coil (Alecci *et al*, 2001 Magn. Reson. Med. 46, 379-385).

To determine the distribution of tissue types, code from the FMRIB Software Library (FSL, available from www.fmrib.ox.ac.uk/fsl/) was utilised. A T_1-weighted structural image of each subject was acquired (3D Inversion Recovery Turbo FLASH, data matrix=256×256, 128 slices, FOV=256×256×192 mm, TR/TE/TI=15/6.9/500 ms, flip angle=15°, 4 interleaves). Brain extraction (Smith 2000 Neuroimage 11, S625) of the structural image was performed followed by tissue segmentation (Zhang *et al*, 2001 IEEE Trans. Med. Imaging 20, 45-47) into the three principal tissue types (grey matter, white matter and cerebrospinal fluid) and rigid-body registration (Jenkinson & Smith 2001 Med. Image Anal. 5, 143-156) to the magnitude-reconstructed spin-echo image from the B_0 map data set.

A further step was applied in order to correct for the spatial variation of EPI signal arising from other sources, predominantly B_1 variations. These effects were modelled as low (up to second) order polynomial modulations of signal intensity, and were fitted to the intensity distribution of the EPI acquired without the mouth shim. This was performed for each tissue type separately, and only in regions exhibiting minimal signal loss artifact, yielding both the B_1 distribution (found to be consistent across tissue types, and in agreement with previous measurements of B_1 inhomogeneity (Alecci *et al*, cited above)), and the relative signal intensity between tissue types (due to differences in T_1, T_2, etc.). Note that this estimation was performed only in regions of minimal signal loss, in order to avoid contamination in the estimation of susceptibility artifacts. The mask defining the region of minimal signal loss artifact was defined as those voxels showing a spatial derivative of the B_0 field in the through-plane (z) direction of less than 0.33 Gm^{-1} as calculated from the associated B_0 map (for a 6mm slice thickness and 30ms TE this is equivalent to a 10% loss of signal at 3 Tesla whilst assuming only a dependency on intravoxel dephasing in the z-

direction that is linear). Finally, the extrapolated polynomial distribution of B_1 intensity for each tissue class was extended into the signal loss affected regions to obtain the ideal reference image.

A map of all voxels that experienced an EPI signal loss greater than 25% with or without the mouth shim present, relative to the ideal reference image, was constructed. Regions of signal loss artifact arising from the ethmoid and sphenoid sinuses, clearly separated within the brain from signal loss artifact arising from other sources (e.g. in the ITCs), were labelled to produce the IFC mask. Similar masks were calculated for 50% and 75% signal loss.

Simulation

To support the experimental results the inventors simulated the effect of the mouth shim on brain B_0 for each subject. The simulation (Jenkinson *et al*, 2002 Proc. Intl. Soc. Magn. Reson. Med. 10, 2325) utilised first order perturbation theory to calculate B_0 within non-conductive objects. The perturbation method enables an estimation to be made of the B_0 compensating effects from a material of complex shape and low magnetic susceptibility ($\chi << 1$).

For each subject, the previously acquired and registered T_1-weighted structural image was used to determine the location of the roof of the subject's mouth and hence the position of the mouth shim. The B_0 distribution due to the presence of the mouth shim only was simulated using the above method at a resolution of 2×2×2 mm (FOV=256×256×256 mm). This was then re-sampled to 4×4×6 mm resolution and linearly combined with the experimental brain B_0 map obtained without the mouth shim (first order perturbation theory allows for linear superposition of B_0). First and second order spherical harmonics were removed to imitate the experimental global brain shim. The resulting B_0 map is termed the simulated brain B_0 map; the difference B_0 map is defined as the result of subtracting the experimental brain B_0 map, obtained with mouth shim, from the simulated brain B_0 map. A small difference map indicates accurate modelling.

For subject E, an additional brain B_0 map was simulated with twice the volume of CNPG (12.2 cm^3) present within the roof of the mouth in order to investigate the effects of an increased quantity of material.

RESULTS

B_0 results are expressed in parts per million (ppm). Within a region of interest, the mean B_0 field deviation is defined as $\overline{\Delta B_0}$, and the B_0 standard deviation as $\sigma(B_0)$.

Table 1 provides experimental B_0 results within the IFC mask of each subject without and with the mouth shim. Considerable improvements in both $\overline{\Delta B_0}$ and $\sigma(B_0)$ are visible in all subjects, the average reductions in these measures being 69% and 28% respectively.

Table 1

Mean deviation and standard deviation of B_0 within the IFC mask of each subject. Experimental results ($B_{0,expt}$) without and with the mouth shim are presented. Results from the difference map ($B_{0,diff}$) between experimental and simulated B_0, both with the mouth shim, are also shown.

Subject	IFC Mask Size	$B_{0,exp}$/ppm				$B_{0,diff}$/ppm	
		No Mouth Shim		Mouth Shim		Mouth Shim	
		ΔB_0	(B_0)	ΔB_0	(B_0)	ΔB_0	(B_0)
A	373	0.392	0.351	0.117	0.228	0.027	0.060
B	395	0.417	0.305	0.052	0.184	0.064	0.084
C	551	0.512	0.381	0.054	0.249	0.047	0.052
D	590	0.395	0.302	0.040	0.193	-0.026	0.092
E	639	0.422	0.383	0.293	0.366	-0.013	0.060
F	745	0.475	0.337	0.261	0.254	0.023	0.040
Average	549	0.436	0.343	0.136	0.246	0.020	0.065

The amount of signal loss artifact within the IFC-masked unwarped EPI images, excluding the most inferior slice, is presented in Figure 14 for each of the six subjects both with and without the mouth shim. Across all subjects, the mean decrease in the number of voxels experiencing greater than 25%, 50% and 75% signal loss when the mouth shim is used was 60%, 68% and 67%, respectively. The same measures in the most inferior slice of the IFC mask provided values of 12%, 12% and –9%, respectively. The relative improvement in the measurements from subject E was less than in the other five subjects.

EPI images of subject C experienced typical signal loss artifact without the use of any passive shims. Brain B_0 maps of subject C without and with the mouth shim are shown in rows (a) and (b) of Figure 15, respectively. They illustrate the marked increase in B_0 homogeneity of the IFC due to the mouth shim with minimal deterioration of B_0 in the rest of the brain. Unwarped EPI images from subject C without and with the mouth shim are shown in rows (a) and (b) of Figure 16, respectively. A re-sampled T_1-weighted structural image, for anatomical reference, is provided in row (d) of Figure 16. A significant reduction in signal loss artifact in the IFC, corresponding to the improvement in B_0 homogeneity in this region, is evident.

In row (c) of Figures 15 and 16 the additional improvements on the B_0 map and EPI arising from use of the ear shims are shown for subject C. An ITC mask was created, analogous to the IFC mask, covering regions of signal loss in both hemispheres arising superior to the mastoid air cells and external auditory canal. Within the ITC mask, present in the fourth through eighth slices of Figure 15 (counting from left to right), the B_0 distribution improves from 0.335 ± 0.329 ppm without to 0.224 ± 0.240 ppm with the ear shims. The decrease in the number of voxels experiencing greater than 25%, 50% and 75% signal loss within the ITC mask is 30%, 34% and 21% respectively. In the more inferior slices of the ITC, outside the ITC mask, the ear shims produce little manifest change in signal loss artifact.

The locally placed passive shims have a minimal effect on B_0 in the rest of the brain following the global shim of brain B_0. For the whole brain, $\overline{\Delta B_0}$ was near zero both

without and with the mouth shim for all subjects, since the global FID was placed on resonance during prescan for both conditions. Due to the small volume of the IFC mask relative to the whole brain (e.g. in images of subject C the brain occupies a volume 31 times larger than the IFC mask) the average improvement in whole-brain $\sigma(B_0)$ due to the mouth shim was small, decreasing from 0.200 ppm without to 0.186 ppm with the mouth shim. The inter-subject standard deviation in the angle of head tilt (transverse-coronal) was 6°, indicating that the subjects were placed in the magnet in a reasonably consistent manner.

Simulation

The simulated B_0 distribution arising from the mouth shim alone is shown in Figure 17. When placed in the roof of the mouth, the large B_0 lobe superior to the shim overlaps with the IFC B_0 inhomogeneity while the smaller lateral B_0 lobe impinges negligibly on the inferior portions of the brain. Residual large-scale B_0 variations present in the brain are removed through subsequent active shimming using first and second order room temperature shim coils.

Information on the difference B_0 map within the IFC mask of each subject is presented in the right-hand column of Table 1. The simulation is shown to well replicate the effect of the mouth shim on B_0 within the IFC. For the six subjects, $\sigma(B_0)$ of the whole-brain difference B_0 maps were 0.058, 0.063, 0.065, 0.061, 0.063, and 0.067 ppm. In comparison to the mean whole-brain $\sigma(B_0)$ with the mouth shim of 0.184 ppm, this result supports the mouth shim simulation model and subsequent B_0 calculation.

Example sagittal views of experimental and simulated brain B_0 maps of subject E, with the mouth shim present, are displayed in rows (b) and (c) of Figure 18, respectively, and demonstrate close agreement. The experimental brain B_0 map of subject E without the mouth shim present is shown in Figure 18(a). The B_0 map of subject E experienced a large initial IFC inhomogeneity and the least improvement from the use of the mouth shim. However, an appreciable reduction in the IFC B_0 inhomogeneity is still visible between

rows (a) and (b) of Figure 18. In Figure 18(d), a simulated B_0 map of subject E with twice the volume of CNPG present in the mouth is shown. Within the IFC mask the B_0 distribution narrowed from 0.422 ± 0.383 ppm, without any CNPG, to 0.293 ± 0.366 ppm with 6.1 cm^3 of CNPG, and to 0.120 ± 0.317 ppm (simulated) with 12.2 cm^3 of CNPG. This indicates that significant further reduction of the IFC B_0 inhomogeneity in subject E is possible with an additional quantity of material. The whole-brain B_0 distribution changed only slightly when the amount of CNPG was doubled, indicating that regions of the brain outside the targeted area would not be significantly adversely affected.

The simulation of the B_0 distribution due to the mouth shim alone, performed at a resolution of 2×2×2 mm, took 332 s using a Compaq Alpha server ES40 (667 MHz Alpha processor). Note that such simulations need only be performed once per passive shim shape/size.

Discussion

A substantial decrease in the mean and standard deviation of IFC B_0 inhomogeneity was evident in all subjects using a single size and shape of mouth shim. Geometric distortion artifact, being proportional to the magnitude of off-resonance frequency, was reduced by an average of 69%. This corresponds to a mean displacement of 2.6 pixels without and 0.8 pixels with the mouth shim within the IFC. The size of signal loss artifact within the IFC mask, excluding the most inferior slice, was also considerably diminished (as shown in Figure 14). In the IFC mask slice nearest to the ethmoid and sphenoid sinuses, the ability of the mouth shim to reduce signal loss artifact is limited due to the high order spatial variation of B_0 adjacent and superior to the air-tissue interface. However, a reduction in geometric distortion is still manifest in this slice.

Images of subject E underwent the least improvement with the mouth shim. This was partly due to the presence of a large IFC inhomogeneity. However, with the B_0 distortion due to the mouth shim roughly proportional to $1/r^3$, the displacement in z (parallel to B_0) between the roof of the mouth and the bottom of the IFC is an important parameter. For subjects A to F, this distance, to the nearest 1.5 mm, was 48.0 , 52.5 , 56.0 , 52.5 , 67.5

and 54.5 mm. The increased mouth-IFC distance in subject E reduced the effectiveness of the standard mouth shim. The effect of doubling the volume of CNPG in the mouth shim for subject E, to compensate for the above disparity, was simulated and is discussed below.

In Figures 15 and 16, the advantageous effect of the mouth shim on images of the IFC of subject C, who experienced a typical signal loss artifact without passive shimming, is apparent. In particular, the region of the EPI image encompassing the orbitofrontal cortex and the anterior portion of the amygdala experiences a substantial gain in signal. With the B_0 inhomogeneity in the IFC diminished, the global brain shim is more able to make B_0 uniform elsewhere in the brain. For example, as observed in rows (a) and (b) of Figures 15, lateral regions of the frontal cortex are more on-resonance with the mouth shim present. Superior areas of the brain are also more homogeneous (not shown). However, the B_0 inhomogeneity arising superior to the frontal sinus, in the anterior portion of the frontal lobe, increases slightly in amplitude due to this decreased IFC shim weighting. This is noticeable in the more superior slices of the EPI images shown in rows (a) and (b) of Figure 16.

The example application of the ear shims to subject C demonstrated an advantageous reduction in EPI susceptibility artifact in the more superior slices of the ITCs. However, at present, the use of the ear shim provides more speculative and less robust results than the mouth shim and does not impact significantly on the more inferior regions of the ITCs.

Simulation

The simulation was shown to model closely the changes in B_0 within the IFC and the whole brain due to the presence of the mouth shim. For example, $\sigma(B_0)$ of the whole-brain difference B_0 map was typically one-sixth of the magnitude of $\sigma(B_0)$ of the whole-brain experimental B_0 map. In Figure 18, it is clear that further improvements in the IFC B_0 homogeneity of subject E, who possesses a greater than average mouth-IFC distance, are possible albeit through a larger quantity of CNPG in the roof of the mouth. A more important point is that optimisation of the location and amount of CNPG comprising the

mouth shim, with constraints imposed through anatomy and comfort, is possible. This can be achieved through utilisation of the B_0 simulation with knowledge of the size of the IFC B_0 inhomogeneity and the geometry of the head. There is, therefore, the prospect of a quick, practical and subject-specific protocol for the application of the mouth shim within an fMRI study.

General Issues

Previous attempts at passively shimming the human brain B_0 have involved the use of ferromagnetic shim components (Jesmanowicz *et al*, 2001 Proc. Intl. Soc. Magn. Res. Med. 9, 617). In order to negate the positive B_0 inhomogeneity arising superior to an air cell, a single ferromagnetic shim must be placed lateral to that air cell. The spatial variation of the shim B_0 inhomogeneity would then be highly dissimilar to the air cell inhomogeneity and would have little beneficial effect. A plurality of ferromagnetic shims can be useful in removing larger scale B_0 inhomogeneities of the brain but is a limited and time-consuming approach towards reducing the high magnitude IFC and ITC inhomogeneities.

A dual-component paramagnetic and diamagnetic implant, using Bismuth (χ=-164 ppm [Schenk 1996, Med. Phys. 23, 815-850]), has been previously suggested to reduce susceptibility artifacts compared to metal-only implants (Chauvel *et al*, 1996 J. Magn. Reson. Imaging 6, 936-938). However, the present novel approach of placing a diamagnetic passive shim inferior to the IFC is shown in this study to be an effective and practical technique for reduction of the IFC B_0 inhomogeneity and the resulting susceptibility artifacts.

The distribution of B_0 with the mouth shim in place is not dependent on EPI sequence acquisition parameters. It is therefore possible to predict, for instance, that a coronally acquired EPI of the IFC, with the majority of signal loss arising due to spatial gradients of B_0 in the anterior-posterior direction, will experience a similar relative reduction in signal loss artifact as presented here for axial acquisition. The level of distortion artifact, being dependent only on the amount of off-resonance and the time between phase encode "blips"

of the EPI sequence, will be identical but in an alternative direction (along the EPI phase encode direction).

When placing a foreign body within the mouth of a volunteer, safety is of prime importance. The possibility of RF heating of the CNPG was investigated and found, through theoretical analysis and calorimetry experiments to be of a safe level. Gradient induced eddy currents within the CNPG material are negligible. CNPG is a non-toxic material and was fully enclosed within a customised mouth mould in this study to ensure hygiene. The polymorph plastic used to construct the mouth mould in this preliminary study is non-hazardous, biodegradable, immensely strong and tough, mouldable at around 60°C and machinable below 30°C. It can be tailored to each individual for comfort and discarded following the study.

The possibility of the CNPG shim altering the coupling between the head coil and the subject was also investigated. Repeated fitting and removal of the mouth shim by the subject produced negligible alterations of less than 1% in the quality factor of the coil. The centre frequency of the coil was not altered. As would be expected by these results the presence of the mouth shim produced no measurable signal loss on spin echo images acquired of the subject.

At present, the construction of the mouth shim is relatively simple in design. The shim is held securely in place through light clasping of the teeth. One out of the six subjects found the presence of the shim in the roof of the mouth uncomfortable. The remaining five subjects, after becoming accustomed to its presence, were at ease. Further design considerations should produce more comfortable and tolerable devices (e.g. through more effective filling of the roof of the mouth). Due to the anisotropic nature of the magnetic susceptibility of CNPG, when the graphite basal plane is not perpendicular nor parallel to B_0 a slight torque is produced on the material. When fitted properly in the mouth, with the CNPG plates close to perpendicular to B_0, the torque is negligible (at 3 T) and not an issue of concern. However, to remove the effect of the torque on the subject entirely the mouth shim could be incorporated within a bite bar arrangement.

The ear shim provided limited benefit in reducing B_0 inhomogeneity in the ITCs. Further investigation into the design and placement of the ear shim may produce enhanced results. In addition, the use of a "brow shim", a piece of CNPG placed adjacent to the eyebrows or on a set of prism glasses worn by the subject, may prove useful in the reduction of B_0 inhomogeneity caused by the presence of the frontal sinus.

Ideally, some form of active shim method (e.g. Wilson *et al*, 2002 Proc. Intl. Soc. Magn. Reson. Med. 10, 1230; Spielman *et al*, 1998 Magn. Reson. Med. 40, 376-382; Gruetter 1993 Magn. Reson. Med. 29, 804-811) must be used together with the presented technique to remove the low-order variations in B_0 produced by the passive shim. Linear dynamic shimming (Blamire *et al*, 1996 Magn. Reson. Med. 36, 159-165) may also be used in conjunction with the proposed technique, thereby further reducing any large-scale slice-by-slice B_0 variations.

Despite the already large improvements in IFC B_0 homogeneity, simultaneous use of other artifact reduction methods will more comprehensively reduce signal loss and geometric distortion artifacts. Gradient compensation methods (Merboldt *et al*, 2000 J. Magn. Reson. 145, 184-191; Frahm *et al*, 1988 Magn. Reson. Med. 6, 474-480; Song 2001 Magn. Reson. Med. 46, 407-411) require several acquisitions with varying slice-select gradient refocusing magnitudes resulting in decreased temporal resolution of an fMRI study. The use of diamagnetic passive shimming should greatly reduce the number of such acquisitions required. The present constraints placed on RF pulse tailoring techniques (Stenger *et al*, 2000 Magn. Reson. Med. 44, 525-531) should also be relaxed when used in conjunction with the proposed passive shimming method. Image unwarping algorithms (Jezzard & Balaban 1995 Magn. Reson. Med. 34, 65-73) will also be more reliable in the presence of B_0 inhomogeneities of smaller magnitude.

This study has covered the use of a single model of mouth shim of simple design. As mentioned above, optimisation in the size and location of the mouth shim, through reliable simulation of B_0, allows for routine use of subject-specific mouth shims within fMRI

studies. With a set of CNPG shims of varying size and shape available to the scanner operator, the inventors here outline a possible protocol for identifying the optimal shim for a subject: (i) a customised mouth mould or bite bar is constructed for the subject; (ii) the subject is placed in position within the scanner and a B_0 map obtained of the whole head; (iii) the optimal shim is found using the presented B_0 simulation code, the acquired B_0 map and further anatomical information from the magnitude-reconstructed B_0 map data; (iv) the subject is brought out from the bore, the chosen CNPG shim is placed in the mouth mould or within the bite bar set-up and this is placed in the mouth of the subject; (v) the subject is returned into the scanner bore, an active shim sequence is performed and the study begun. This should increase the length of the study by no more than about five minutes.

A more optimal approach would be to determine also the most favourable shape of the mouth shim on a subject-by-subject basis. This could be performed by designing a shim that possesses the appropriate inverse harmonic deconvolution of the measured B_0 field in the IFC. However, the mouth shim design is severely constrained by what the subject will find comfortable to have in his or her mouth. In addition, as has been shown in this study of subjects with a wide range of B_0 inhomogeneity magnitudes, large improvements in IFC B_0 homogeneity are to be gained even without tailoring the volume of CNPG to each subject.

Example 5

The previous examples demonstrated that the use of a single, strongly diamagnetic, passive shim in accordance with the invention significantly improves the homogeneity of the static magnetic field (B_0) and, as a result, reduces susceptibility artifacts within the IFC. In this example the inventors analysed the effect of utilising a passive shim in accordance with the invention in a BOLD fMRI study of the IFC. Simulations of B_0 instabilities within the IFC resulting from subject head motion were performed and analysed in order to calculate the effects of the shim on the temporal variance of an EPI time series. In addition, an fMRI experiment involving a hypercapnia challenge was performed to demonstrate the potential gain in effective BOLD contrast within the IFC due to the presence of the passive shim.

Transient changes in the B_0 distribution within the brain between the repeated acquisitions of an EPI time series have been shown to alter the local magnitude of geometric distortion artifact on a scan-to-scan basis (Jezzard *et al*, 1999 Hum. Brain Mapp. 8, 80-85; Hutton *et al*, 2000 NeuroImage 11, S495). This can result in increased variance within BOLD fMRI data and in a subsequent decline in sensitivity to, and specificity for, brain activations. Assuming that the scanner itself is stable, such transient changes in B_0 are likely to result from either: (i) fluctuations in the B_0 inhomogeneity distribution throughout the brain resulting from inter-scan subject head motion (Andersson *et al*, 2001 NeuroImage 13, 903-919) that lead to locally fluctuating geometric distortion even after perfect realignment using rigid-body or affine registration algorithms, or (ii) movement of objects close to the imaging region that alter the magnetic field distribution in the slices under study, also leading to locally fluctuating geometric distortion. Such moving objects include the chest and diaphragm, as occurs during respiration (e.g. Raj *et al*, 2001 Phys. Med. Biol. 46, 3331-3340); and the tongue and jaw when swallowing or in certain language tasks (Birn *et al*, 1998 Magn. Reson. Med. 40, 55-60).

A potential concern in the use of an intra-oral passive shim was the possibility that its presence could supplement the known sources of transient B_0 changes within the IFC. Since the passive shim is securely held within the roof of the mouth through use of a customised mouth mould (see below), the contribution to B_0 field fluctuations arising from relative movement between the device and the brain is likely to be negligible. With regard to the effects of small head motions during the fMRI scanning session, it was not clear whether transient B_0 variations within the IFC would increase or decrease with the passive shim in place. Although the B_0 distribution induced within the IFC by the passive shim is similar in form to that induced by the ethmoid/sphenoid sinuses, the larger distance between the shim and IFC implies that rotation of the head around the *x*-axis (left-right) or *y*-axis (anterior-posterior) would result in a greater displacement of the shim relative to the IFC, and hence to an amplified change in IFC B_0 distribution. Alternatively, the superposition of B_0 inhomogeneities from the sinuses and the intra-oral passive shim may serve to reduce such transient effects.

Example 5.1

B_0 Simulations

In order to determine the extent of any contribution arising from the presence of a mouth shim to instabilities in the fMRI time course, a number of numerical simulations were performed. Various effects of head motion were considered. These included consideration of the effects of fluctuations in local geometric distortion (resulting from local changes in the B_0 field), and consideration of the effects of fluctuations in local signal intensity (resulting from local changes in the intrinsic intra-voxel B_0 field gradient). Simulations were conducted both for a model that included an intra-oral CNPG passive shim, and for a model that did not include a shim. It was assumed that for a well shimmed bare magnet the inherent brain B_0 distribution arises either due to the difference in magnetic susceptibility between tissue and air (case of no shim) or additionally due to the presence of the CNPG shim (case of shim present). With this assumption, simple translations of the head model in any direction would cause no change in B_0 distribution and were not considered.

Rotations of the head model were performed about the three Cartesian axes, R_x (left-right), R_y (posterior-anterior) and R_z (inferior-superior), and the resulting B_0 distribution arising from the air-tissue interfaces within the head were simulated. Note that the rotations were accomplished by altering the theoretical angle of the external B_0 field relative to a fixed model of the head. In this way interpolation errors that might result from numerical rotation of the head model were minimised.

The head model was constructed from a 1.5×1.5×1.5 mm resolution proton density-weighted structural MR image covering the whole head and neck of a normal volunteer, as illustrated in Fig. 19a and shows outlines of the brain mask and IFC mask superimposed. The segmentation of the head model into regions of tissue and air was aided by reference to a registered 2.0×2.0×2.0 mm resolution CT head image, yielding a map of the regions of differing magnetic susceptibility. All voxels in this magnetic susceptibility (χ) map were assigned a value of either 0.4×10^{-6} (air) or -9.1×10^{-6} (tissue). Further segmentation of the head model into different tissue types (including bone) was not performed due to the

relatively small susceptibility differences between the different tissue structures. Figure 19b shows a medial sagittal cross-section of the susceptibility map, and also shows the position of the CNPG shim (shown in white) in the roof of the mouth. Air spaces are black, and tissues shown in grey. For the simulations that include the CNPG shim, a volume of 5.69 cm^3 of CNPG (Minteq International Inc., PA) was used. Perpendicular to the graphite basal plane, a susceptibility value of -565×10^{-6} was assumed, as was recently measured using a SQUID magnetometer.

Maps of the magnetic field within the head model were generated for various relative angles between the model and the direction of the external magnetic field. In all, fifteen orientations were simulated about each of the three principal axes. The set of angles used was $\theta = \{-4.0°, -3.5°, -3.0°, -2.5°, -2.0°, -1.5°, -1.0°, 0.0°, 1.0°, 1.5°, 2.0°, 2.5°, 3.0°, 3.5°, 4.0°\}$. A first order perturbation method (Jenkinson *et al*, 2002 Proc. Intl. Soc. Magn. Reson. Med. 10, 2325) was used to calculate each of the resulting magnetic field maps, yielding a set of B_0 field maps, termed $B^j_{0,\theta}$ where j specifies the rotation axis $j \in \{x, y, z\}$. The perturbation method enables an estimation to be made of the effect on the B_0 distribution from a non-conducting material of complex shape and low magnetic susceptibility provided $\chi \ll 1$, which is valid for all compartments of the susceptibility model.

First and second order spherical harmonic B_0 variations were removed from the brain region of $B^j_{0,0°}$, the unrotated B_0 distribution, in order to simulate a global brain active shim. Those spherical harmonic variations were then removed from all $B^j_{0,\theta}$ such that the effects of the global brain active shim remained constant.

Once the set of B_0 maps had been calculated a number of effects were considered as follows:

(i) the B_0 field difference between successive rotations about each of the axes:

$$\Delta B^{j}_{0,\theta i} = [B^{j}_{0,\theta i+1} - B^{j}_{0,\theta i}] \cdot \frac{1}{(\theta_{i+1} - \theta_{i})} . \qquad [1]$$

This measure represents the amount of local geometric distortion that occurs during small changes in the angle of the head with respect to the external magnetic field. Note that all B_0 field maps are effectively pre-registered to one-another as part of the simulation, thus accounting for the step of head motion registration that is typically applied as part of most fMRI post-processing strategies.

(ii) the signal change induced by local mis-registrations in echo planar images as a result of variations in local geometric distortion as the head is tilted. The local geometric distortions were simulated using the field shift information derived in step (i) by applying an appropriate geometric distortion algorithm to *in vivo* EPI data collected on our scanner. In this way the locally distorted image, I_θ, could be derived at each angle, along with an estimate of the fractional change in distortion-related signal that accompanies small tilts of the head. This latter measure is calculated as:

$$\Gamma^{j}_{\theta i} = \frac{\Delta I^{j}_{\theta i}}{I^{j}_{\theta i}} = 100\% \cdot \frac{(I^{j}_{\theta i+1} - I^{j}_{\theta i})}{I^{j}_{\theta i}} \cdot \frac{1}{(\theta_{i+1} - \theta_{i})} . \qquad [2]$$

(iii) the difference in the slice-direction B_0 field gradient between successive rotations about each of the axes. The field gradient, G_z, was calculated as the local value of the linear field gradient in the z (slice) direction for each value of θ and for each rotation axis. Any local changes in G_z will represent a significant contribution to intra-voxel dephasing, and hence signal loss. Note that in order to properly calculate the G_z values the relevant $B_{0,\theta}$ map must first be rotated by the angle θ. The calculated G_z maps were then rotated back to account for the head motion correction step. A calculation similar to step (i) was then performed on the resulting data, yielding a measure $\Delta G^{j}_{z,\theta i}$.

(iv) an estimate of signal loss resulting from local fluctuations in G_z. The values of G_z were taken from the results of step (iii), followed by application of a signal loss equation given

by $I=I_0\text{sinc}(\gamma G_z z_{thk} TE/2)$, where the slice thickness, z_{thk}, was assumed to be 6 mm and the echo time TE was assumed to be 30 ms. A calculation similar to step (ii) was then performed on the data.

All the above analyses were conducted both for the case of the model with the CNPG shim in place, and for the case of the CNPG shim absent. Subsequently, masks of the brain and the IFC were constructed, as detailed in the Appendix, and mean values of the above parameters were calculated within the brain mask and IFC mask.

Results

Simulated results of $B^j_{0,0^\circ}$ (the B_0 field arising from the unrotated head model) are presented for the model without the CNPG shim (Fig. 20a) and with the CNPG shim (Fig. 20b). The improvement in B_0 homogeneity within the IFC region due to the presence of the mouth shim is clearly visible. Example difference B_0 maps evaluated close to $\theta=0^\circ$, $\Delta B^j_{0,0^\circ}$, are also illustrated in Figs 20c to 20f for rotations about R_x and R_y. As the main B_0 field lies along R_z, rotations about this axis leave the B_0 field unchanged and are not considered here. However, as will be shown, rotations about R_z do still contribute to the temporal instability of an echo-planar image series. In Figures 20a-f, the left hand column shows midline sagittal views, the middle column coronal, and the right hand column axial views, respectively. The white cross hairs indicate the location of the slices. The limits of the B_0 range in Figs. 20a–20b is ±1.0 ppm, and for the $\Delta B^j_{0,0^\circ}$ range in Figs. 20c–20f is ±0.02 ppm/degree. These ranges would correspond to geometric distortions in the phase-encode direction of an echo-planar image of 6.0 voxels and 0.12 voxels/degree, respectively, for the EPI sequence described elsewhere. Results from the original head model, with no CNPG shim, are shown in Figures 20 a, c and e, whilst results obtained using a shim in accordance with the invention are shown in Figures 20b, d and f.

Graphs plotting the values of $<|\Delta B^j_{0,\theta}|>$ in the IFC mask and brain mask (see "Appendix") at other values of θ are presented in Figs 21a and 21b, respectively. The graphs show that within the IFC mask (Fig. 21a) the presence of the CNPG shim versus no shim decreases the

magnitude of the field distortions for rotations about R_y. For the case of rotations about R_x there is no significant difference with the shim present versus absent, although there is a shift in the absolute angle at which the effect of small tilts is minimised. Figure 21b shows that there is no significant difference within the brain mask for the $<|\Delta B^j_{0,\theta}|>$ measure with and without the CNPG shim, although again there is a shift in the minimum position for R_x rotations.

Graphs plotting the value of $<|\Delta\Gamma^j_\theta|>$ within the IFC mask and the brain mask are shown in Figs 21c and 21d, respectively. Results for both without and with a CNPG shim present and for rotations about each of the three Cartesian axes are shown. The plots are more complex than for the field shifts alone, since the calculated values depend on the details of the grey/white matter interfaces, along with other image contrast boundaries. Figure 21c shows that the simulations indicate there is expected to be a significant decrease in the image intensity fluctuations within the IFC mask when then CNPG shim is present (filled symbols versus open symbols). In the case of the brain mask (Fig. 21d) there is a small degradation in the measure of $<|\Delta\Gamma^j_\theta|>$ throughout the brain. Interestingly, rotations about R_x produce the largest change in EPI signal and the value of $<|\Delta\Gamma^x_\theta|>$ is smaller with the head tilting forwards (+ive θ) than with the head tilting backwards (–ive θ). This is an important result to contrast with previous investigations that attempted to identify the optimum angle of head tilt that minimises susceptibility artifacts alone (Heberlein & Hu, 2001, Proc. Intl. Soc. Magn. Res. Med. 9, 1157).

Figure 22 shows the simulation results when considering fluctuations in the spatial derivative of the magnetic field in the slice direction (G_z). Figures 22a and 22b show simulated data that indicate the magnitude of the G_z field gradients for the case of $\theta=0°$, both without (Fig. 22a) and with (Fig. 22b) a CNPG shim present. Figures 22c–4f show $\Delta G^j_{z,\theta}$ difference maps evaluated close to $\theta=0°$ for rotations about R_x (c,d) and R_y (e,f), both without and with a CNPG shim present. The maps indicate in each case an improvement when the CNPG shim is present. In Figures a, b the range is –0.4ppm/cm to 0.4ppm/cm. In Figures c-f the range is –0.015ppm/cm/degree to 0.015ppm/cm/degree.

Results in the absence of the passive shim are shown in Figures 22 a, c and e. Results obtained with the mouth shim are shown in 22b, d and f. The white cross hairs indicate the location of the slices.

Plots of $< | \Delta G^{j}_{z,\theta} | >$ are shown in Fig. 23 evaluated within the IFC mask (Fig. 23a) and the brain mask (Fig. 23b). These show that the presence of a CNPG shim reduces the overall magnitude of anticipated fluctuations in G_z within the IFC mask, and has no significant effect on the overall fluctuations within the brain mask. Also shown in Figs. 23c and 23d are the results the calculations of fluctuations in intravoxel dephasing, evaluated using the signal loss model. Those results mirror the raw field gradient calculations, showing significant reductions in signal fluctuations within the IFC mask when the CNPG shim is present, and an insignificant effect when evaluated over the brain mask. (In Figures 23a-d, plots with shim are filled symbols, empty symbols are plots without shim; R_x = squares, R_y – triangles).

From these results, the inventors conclude that for a specified amount of head motion the presence of a shim in accordance with the invention would improve rather than degrade the temporal stability within the IFC of an EPI time series. However, the temporal stability of EPI signal within the global brain would probably decrease slightly through the pixel misregistration mechanism illustrated in Fig. 21d.

Example 5.2

Hypercapnia Experiment

In order to assess the success of the CNPG shim in recovering effective BOLD contrast we conducted an initial BOLD fMRI study involving a hypercapnia challenge. This allowed a quantitative assessment to be made of the improvement in BOLD sensitivity within the IFC produced by the intra-oral passive shim. Hypercapnia challenges have been used in previous studies since they result in a robust T_2*-weighted BOLD contrast that is produced globally within cerebral grey matter (Rostrup *et al*, 2000 NeuroImage 11, 87-97; Corfield *et al*, 2001 NeuroImage 13, 1207-1211).

A single male subject (age 26 years) was studied, following informed consent, and in compliance with local ethical committee requirements. The intra-oral diamagnetic passive shim used in the B_0 simulation above was fully enclosed within a customised mouth mould of the subject to form a "mouth shim"; the graphite basal plane of the CNPG shim being perpendicular to the B_0 field. The subject mouth mould provided a safe, hygienic and comfortable fit within the roof of the mouth. The mould extended beyond the upper set of teeth at the front and sides of the mouth to ensure that, with the jaw lightly closed, the CNPG shim was stable and secure.

The experiment was performed using a 3T Varian Inova spectrometer (Varian Inc., Palo Alto, CA) fitted with a Magnex SGRAD head gradient coil (Magnex Scientific Ltd., Oxfordshire, UK). First and second order room-temperature shim coils are provided with the system, and a quadrature birdcage transmit/receive head coil was used.

With a mouth shim in place, a GE EPI sequence was used to acquire axial BOLD T_2^*-weighted images of the whole brain during alternating exposure to 5% inspired CO_2 and medical air. Five 90s periods of hypercapnia and five 90s periods of breathing air resulted in a 15 min paradigm. A series of 303 functional images were acquired with the following parameters: data matrix = 64×64, 24 slices, FOV = 256×256 mm, slice thickness = 6 mm, TR/TE = 3000/30 ms, readout bandwidth = 100 kHz. The imaging study was subsequently repeated without the mouth shim in place.

Measurements were made of mean EPI signal intensity ($<I_{EPI}>$) and mean BOLD sensitivity index ($<BSI>$) within both a brain mask and an IFC mask. Maps of $<BSI>$ were calculated using the method described by Deichmann *et al*, (2002 Proc. Intl. Soc. Magn. Res. Med. 10, 1414). Mean absolute B_0 offset ($<|\Delta B_0|>$) and mean absolute slice-direction B_0 field gradient ($<|G_z|>$) were also calculated within both masks from independently acquired B_0 maps (acquired without and with the mouth shim present). Coefficient of Variation maps, CV%, were constructed for both time series (without and with the mouth shim) by dividing a calculated standard deviation image by the mean image and expressing the result as a percentage. The I_{EPI}, BSI and CV% maps were unwarped

before the measures were calculated to ensure correspondence between these maps and the defined masks.

Results from the hypercapnia challenge, without and with the mouth shim in place, are presented in Fig. 24a-f. Sagittal (left hand column), coronal (middle column) and axial (right hand column) images of experimental brain B_0 maps (a,b), BOLD sensitivity index maps (c,d) and *z* statistic activation maps (e,f) are displayed. The hypercapnia reactivity maps shown in Figs. 24e and f reveal large portions of the brain, predominantly regions of grey matter, with a statistically significant change in BOLD signal during hypercapnia. Results with the shim (b,d and f) may be compared to those obtained without the shim (a,c and e). In Figures a and b, the B_0 offset range is −1.0ppm (white) to + 1.0 ppm (black). The BOLD sensitivity scale in Figures c and d begins at zero. In Figures e and f, the *z* statistic range is from 2.3 to 10.0.

The benefits of the mouth shim to B_0 homogeneity, BOLD sensitivity and BOLD activation in the IFC are clearly visible in Fig. 24. Quantitative measures, calculated within both brain and IFC masks, of B_0 homogeneity, the magnitude of susceptibility artifacts and the amount of temporal instability within the EPI time series are presented in Table 2. It can be seen that within the brain mask the mouth shim has a limited impact on all these measures, since the mouth shim only affects brain regions in its proximity. Indeed, within the IFC mask, $<|B_0|>$ is reduced by 68%, <BSI> is increased by 52% and <CV%> is diminished by 25% due to the presence of the mouth shim.

Table 2

Quantitative results from the hypercapnia experiment, without and with a CNPG shim.

Mask	Shim Present	$<\|B_0\|>$ / ppm	$<\|G_z\|>$ / ppm m^{-1}	$<I_{EPI}>$ / a.u.	<BS> / a.u.	<CV%> / %age
Brain	No	0.1095	8.43	9198	3014	4.074

IFC	Yes	0.1091	8.19	9535	3187	4.131
	No	0.5080	31.38	5796	1801	7.994
	Yes	0.1646	16.30	8356	2735	6.024

The results indicate that the presence of a CNPG shim does not adversely affect the temporal stability of the EPI time series, and indeed leads to some improvement within the IFC mask. In practice, translation of the head will also cause changes in B_0 distribution within the brain as a result of an inhomogeneous B_0 field within the scanner bore. However, the magnitude of such B_0 changes is calculated to be substantially smaller within the IFC than those due to head rotation. Also, these effects would be identical whether or not the mouth shim was in use.

The use of a "brow shim", an element of CNPG material placed on the lower portion of the brow, has been found to substantially reduce B_0 inhomogeneity within the anterior portion of the IFC arising from the frontal sinus. However, due to the relatively large distance between a brow shim placed on skin surface and the centre of the brain, it is anticipated that the temporal stability of EPI signal in this area could be compromised by the brow shim in the presence of significant rotation of the head about R_x. Within the IFC the B_0 homogeneity can, if necessary, be further refined through concurrent use of local active shimming methods or by use of other susceptibility artifact reduction methods in combination with a shim in accordance with the invention.

At higher B_0 strengths ($>3T$), the magnetic susceptibilities of air, tissue and CNPG remain approximately unchanged. This implies that the relative improvements in B_0 homogeneity and susceptibility artifacts at higher field strengths should be comparable to the outcome of this study at 3T. Indeed, due to the increased magnitude of susceptibility artifacts at higher B_0 strengths, it is anticipated that the use of an intra-oral passive shim will greatly benefit studies of the IFC using MR techniques at these elevated fields.

For this study, the intra-oral passive shim was not optimised on a subject-by-subject basis. Through further refinement of the passive shim, and utilisation of an accurate and reliable optimisation protocol to determine the most favourable shim design and volume for a particular subject, further B_0 homogeneity improvements within the IFC are attainable.

To summarise, the inventors have simulated the variation of B_0 within the IFC and the global brain due to rotation of the head, and have applied the results to an investigation into the effects of varying geometric distortion and signal loss artifact on EPI time series. In addition to reducing IFC susceptibility artifacts, the presence of a passive shim in accordance with the invention is predicted to improve the temporal stability within the IFC of an EPI time series for a specified amount of head motion. Through fMRI analysis of a subject performing a hypercapnic challenge it was demonstrated that an intra-oral passive shim increased the sensitivity to BOLD activations within the IFC.

APPENDIX

The aim of the intra-oral passive shim is to improve B_0 homogeneity, and consequently susceptibility artifacts, especially within the IFC region of the brain. However, it is also important to maintain image quality within other brain areas. In order to evaluate these two objectives masks of the IFC and the brain were constructed for each data set.

Brain masks were generated automatically using the Brain Extraction Tool (Smith, 2002 Hum. Brain Mapp. 17, 143-155). The IFC mask was automatically generated from B_0 information, rather than being anatomically defined. It encompasses those regions of high through-plane (z direction) B_0 gradient within the brain resulting from, and lying superior to, the ethmoid and sphenoid sinus. The IFC mask therefore also typically includes anterior regions of the amygdala.

To generate the IFC mask, the spatial gradient of the subject B_0 map in the z direction (G_z) was calculated and thresholded at 0.047 mTm^{-1}. For a GE echo-planar image at 3 T with a slice thickness of 6 mm and echo time of 30 ms this cut-off point is equivalent to a 20% loss in signal, assuming a dependency on intravoxel dephasing in the z-direction that is linear

(correct to first approximation). An erosion and dilation step with a 3 voxel kernel element was performed.

The IFC mask was then distinguished from adjacent temporal lobe regions of B_0 inhomogeneity through the determination of the voxel, within the medial 5 cm of the brain B_0 map, that possessed a B_0 value with the greatest deviation from zero. In the present studies, this point was found consistently to lie within the orbito-frontal lobe, directly superior to the ethmoid/sphenoid sinus. The final isolated IFC mask was formed by the removal of brain regions that were not contiguous with this point of greatest off-resonance.

CLAIMS

1. A method of obtaining magnetic resonance data regarding a sample, the method comprising the steps of:

a) placing the sample within a suitable high flux density magnetic field, which field is substantially homogeneous prior to introduction of the sample; and wherein the presence of the sample causes local inhomogeneities in the magnetic field; and

b) causing to be present, adjacent to the sample, a passive shim comprising sufficient amount of a highly diamagnetic substance as to reduce the inhomogeneity in the magnetic field caused by the sample.

2. A method according to claim 1, wherein the highly diamagnetic substance has a magnetic susceptibility of –200ppm or less.

3. A method according to claim 1 or 2, wherein the highly diamagnetic substance has a magnetic susceptibility of –300ppm or less.

4. A method according to any one of claims 1, 2 or 3, wherein the highly diamagnetic substance has a magnetic susceptibility of –400ppm or less.

5. A method according to any one of the preceding claims wherein the sample is a human or animal subject.

6. A method according to any one of the preceding claims, wherein the obtained data are used to produce images of the brain or part thereof.

7. A method according to any one of the preceding claims, the method comprising the use of at least one passive shim comprising a highly diamagnetic substance, and at least one additional passive shim which may be diamagnetic (preferably highly so), paramagnetic (preferably highly so) or ferromagnetic.

8. A method according to any one of the preceding claims, wherein the passive shim comprising the highly diamagnetic material is located at one of the following positions: in the mouth; on or below the brow; and in, on or adjacent to the ear lobe and/or external auditory canal.

9. A method according to any one of the preceding claims wherein the passive shim comprising a highly diamagnetic substance is incorporated in or otherwise attached to a positioning guide.

10. A method according to claim 9, wherein the positioning guide takes the form of a gumshield, bite bar, headphone, earplug or other frame for attachment to the subject.

11. A method according to any one of the preceding claims wherein the obtained magnetic resonance data are used in a method of determining the presence or absence of a pathological condition in a subject, or to analyse the functioning of the brain or part thereof in a healthy subject.

12. A method according to any one of the preceding claims wherein the passive shim is provided with a disposable covering, so that the shim is reusable.

13. A method according to any one of the preceding claims wherein the passive shim is ergonomically shaped and dimensioned so as to minimise discomfort to a subject using the shim.

14. A shim positioning device, the device comprising a passive shim comprising a highly diamagnetic material, and means for positioning, and preferably retaining, the passive shim in a particular location relative to the subject.

15. A shim positioning device according to claim 14, comprising a gumshield, bite bar, headphone, earplug or a frame for engagement with or attachment to a subject's head.

16. A method according to any one of claims 1-13 substantially as hereinbefore described.

17. A shim positioning device according to claim 14 or 15 substantially as hereinbefore described.

18. A passive shim comprising highly diamagnetic material, suitable for use in accordance with the method of any one of claims 1-13.

19. A passive shim according to claim 18, dimensioned so as to be comfortably locatable within the mouth of a human subject.

20. A passive shim according to claim 18 or 19, provided with a disposable covering.

21. A passive shim substantially as hereinbefore described and as shown in the accompanying drawings.

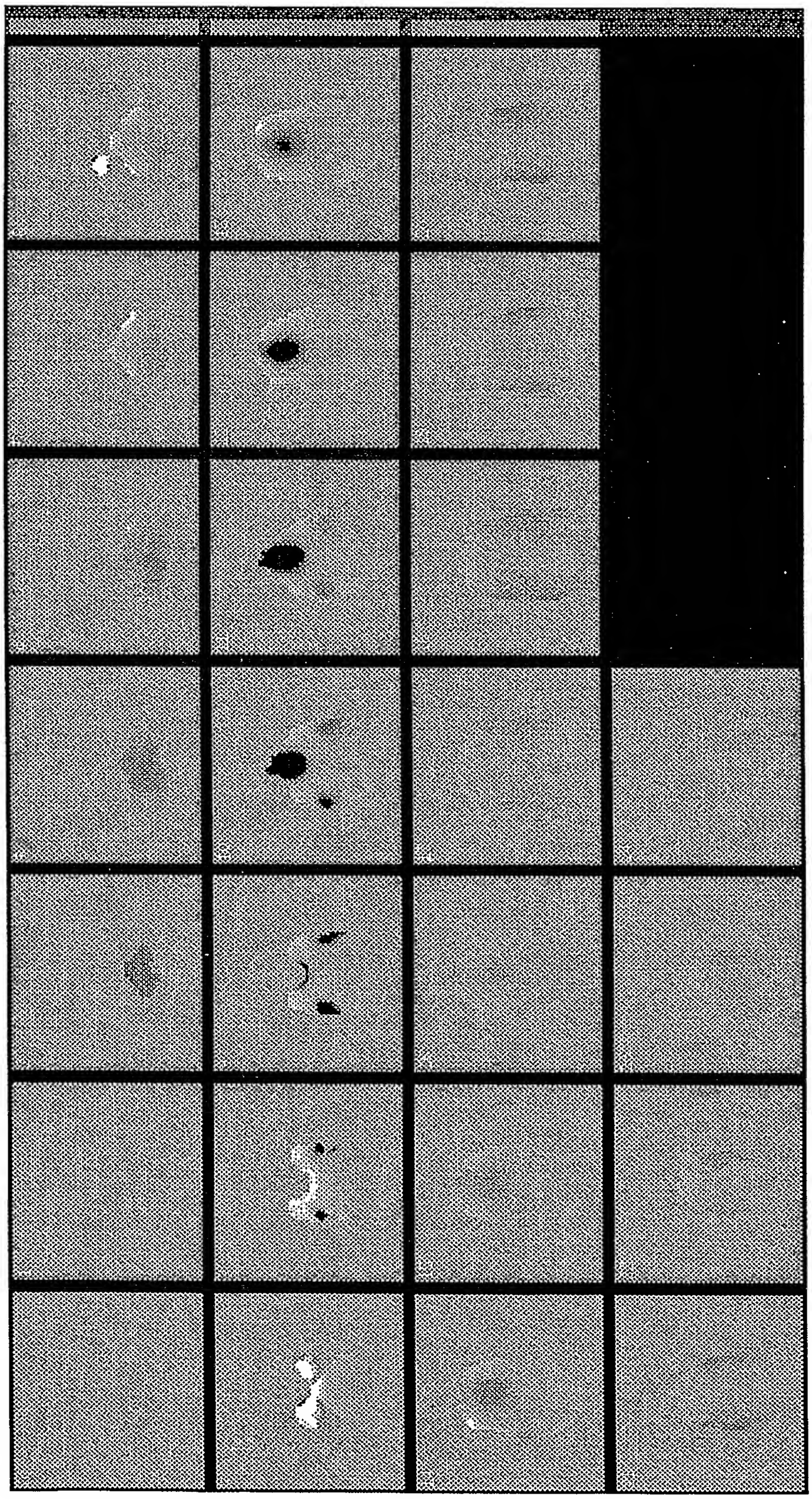

Fig. 1

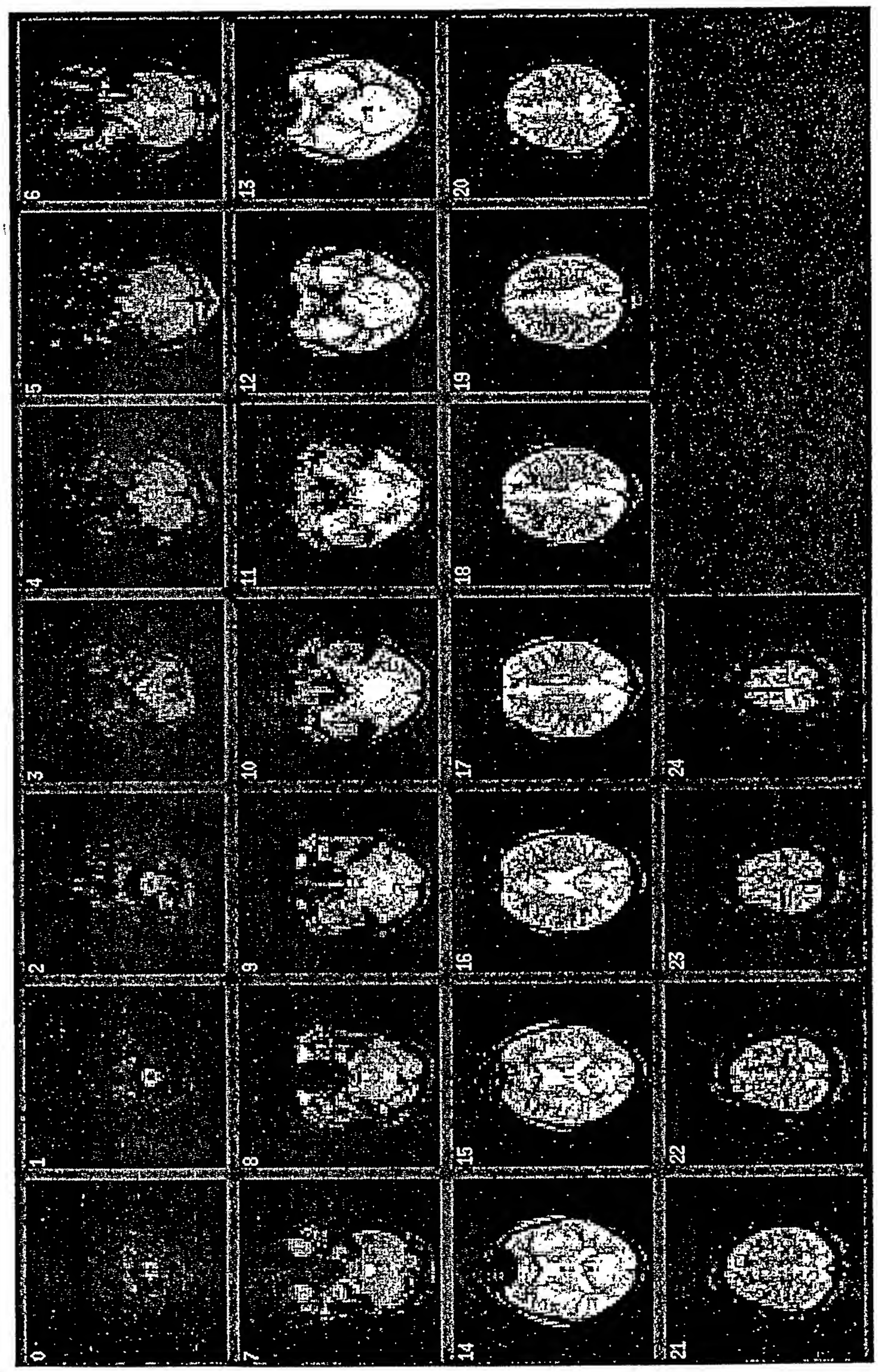

Fig. 2

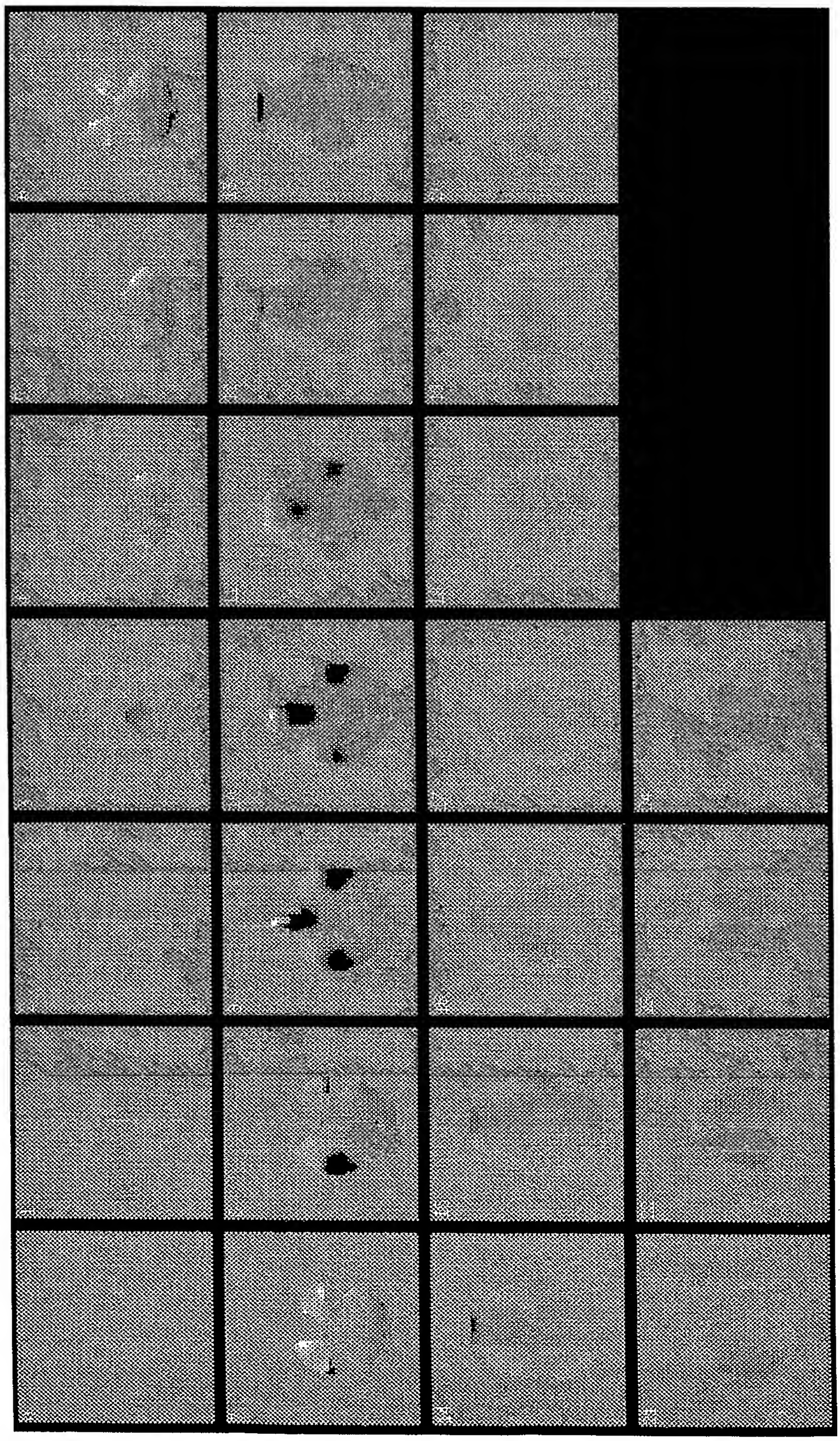

Fig. 3

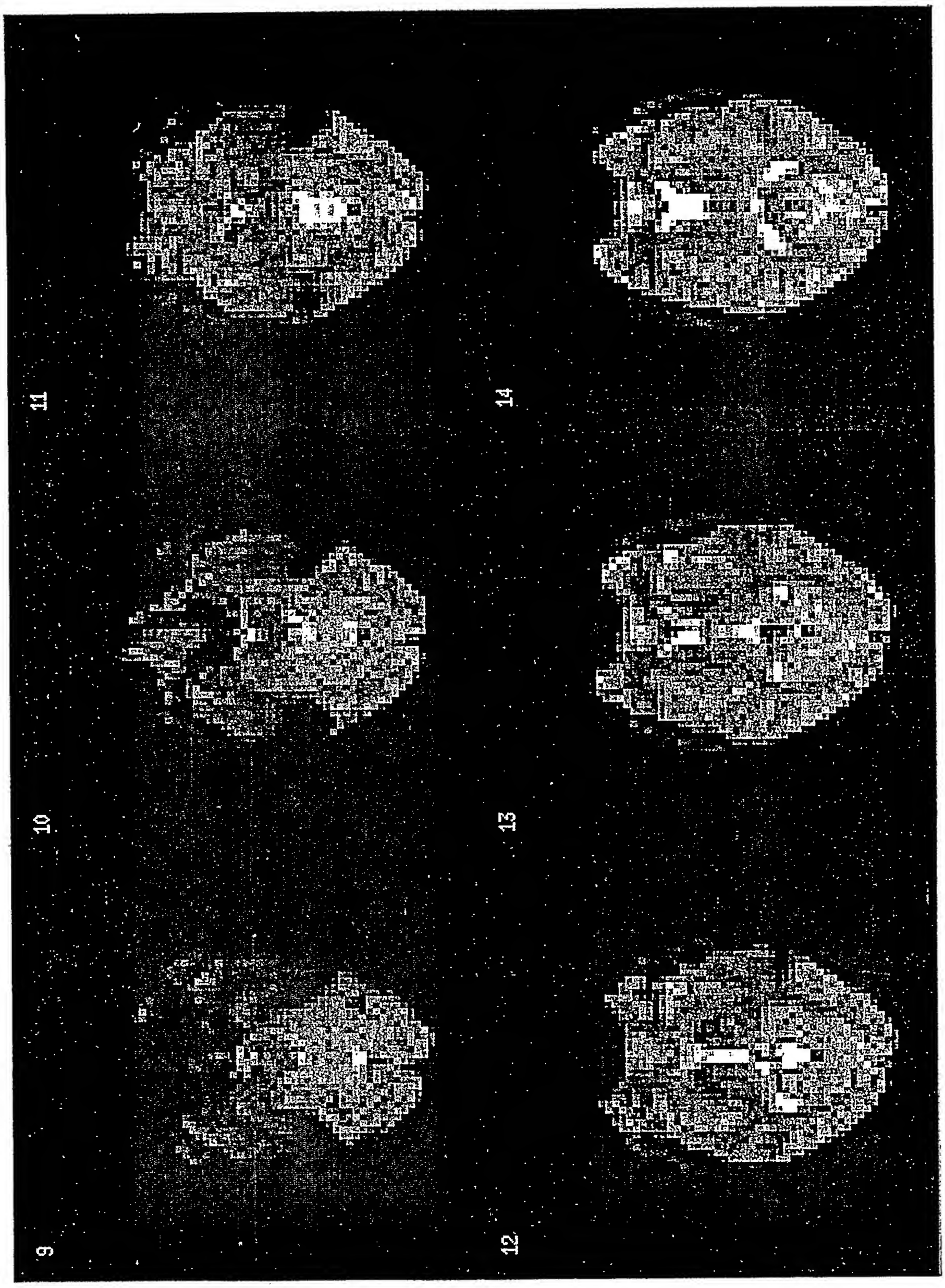

Fig. 4

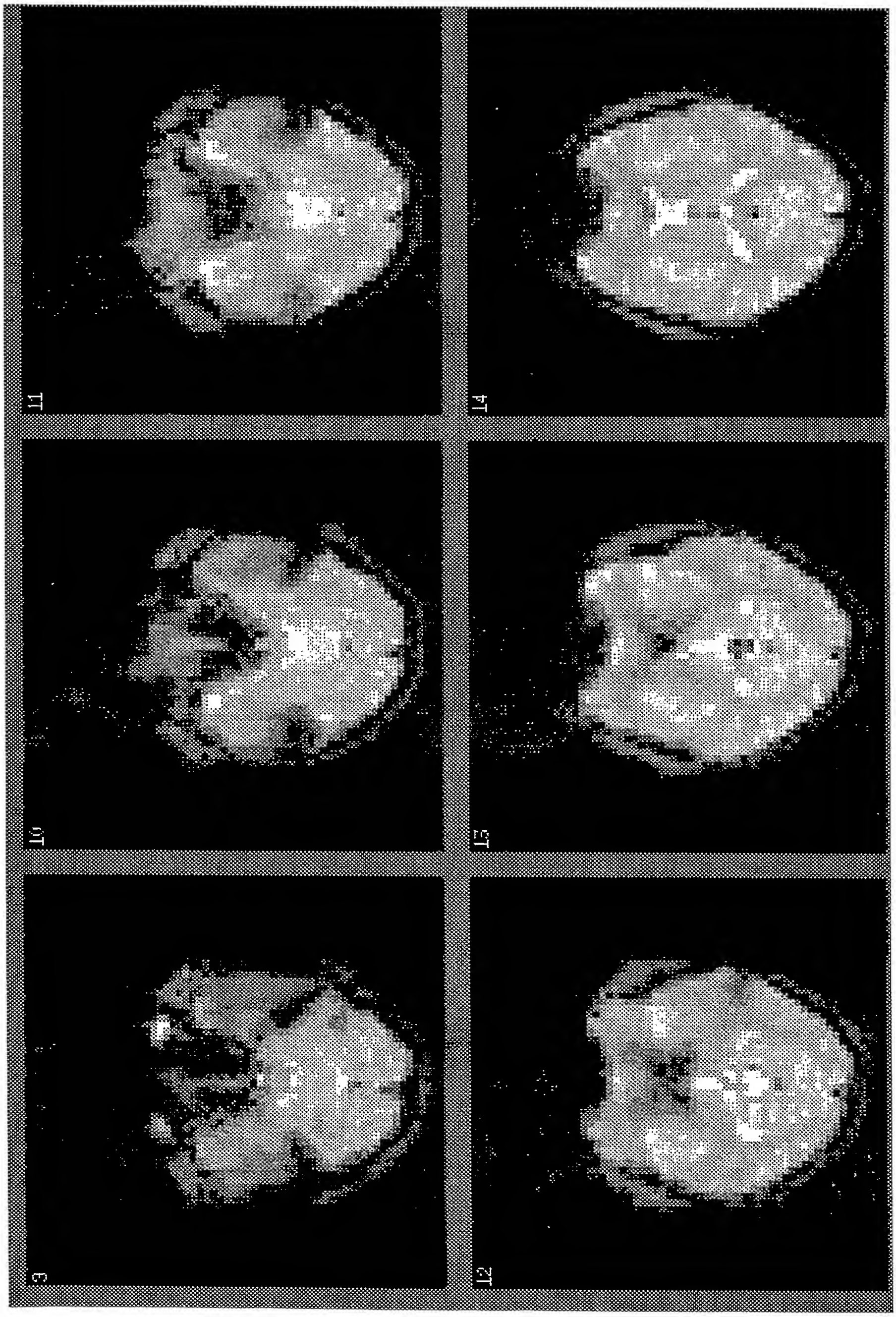

Fig. 5

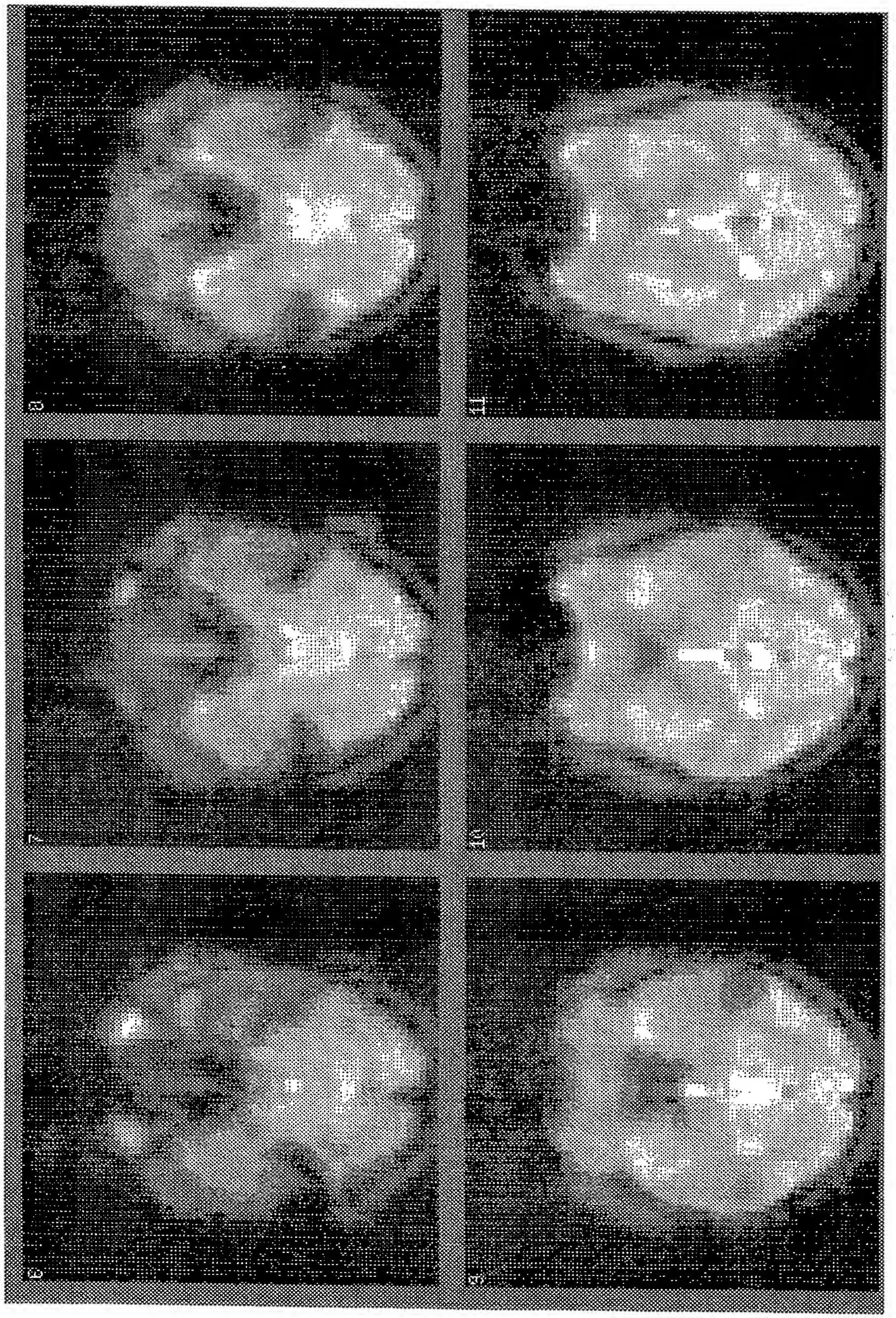

Fig. 6

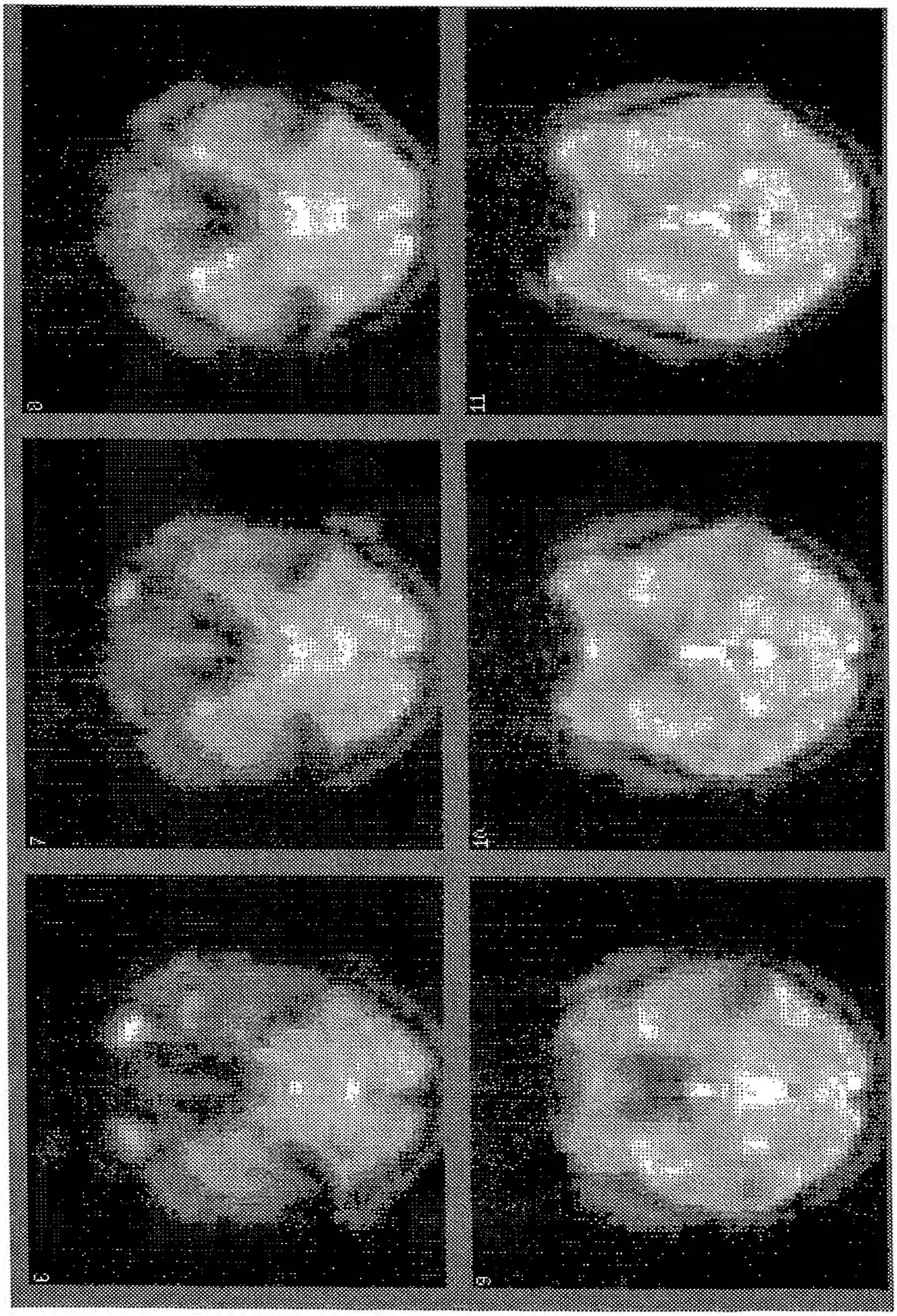

Fig. 7

8/26

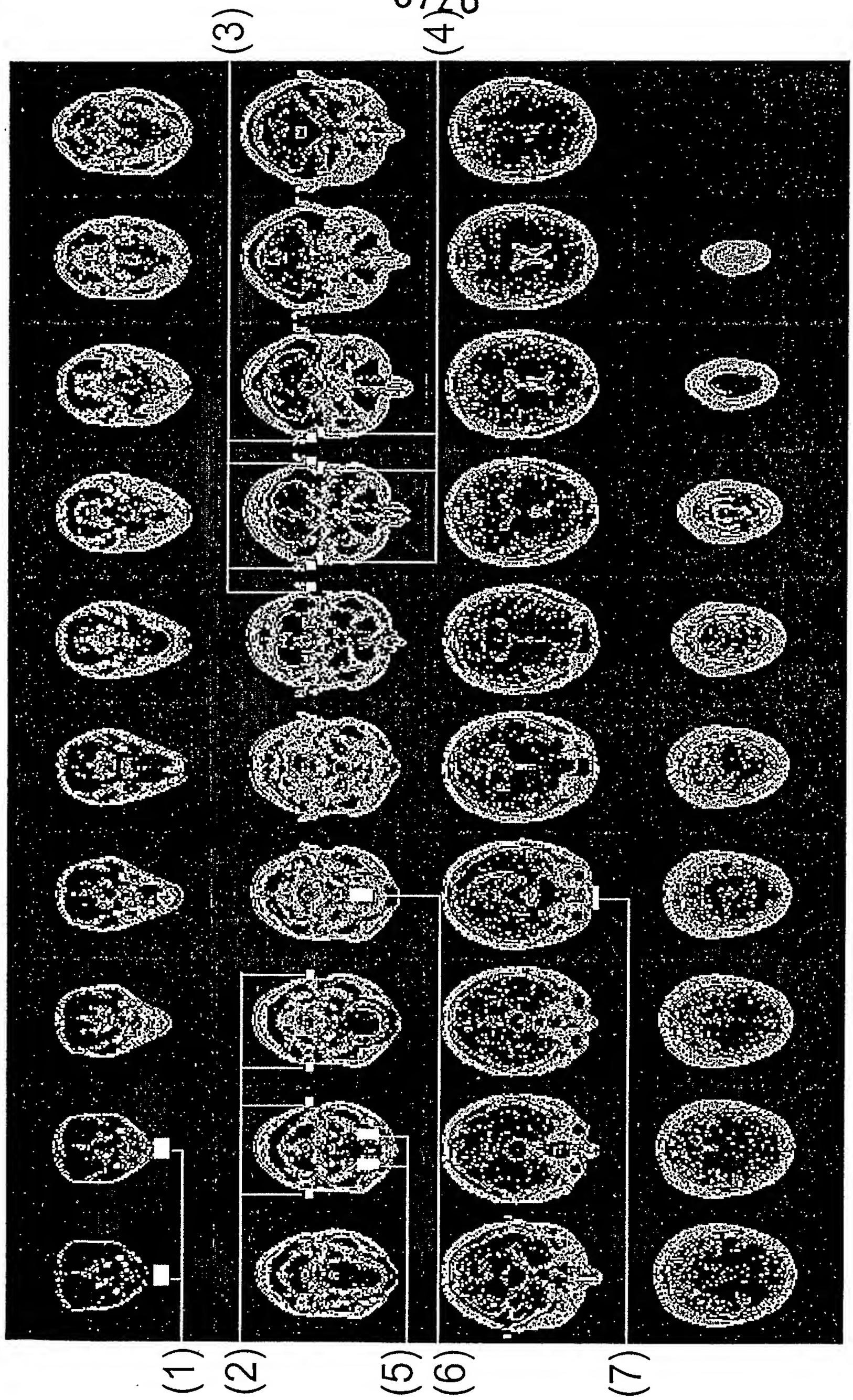

Fig. 8

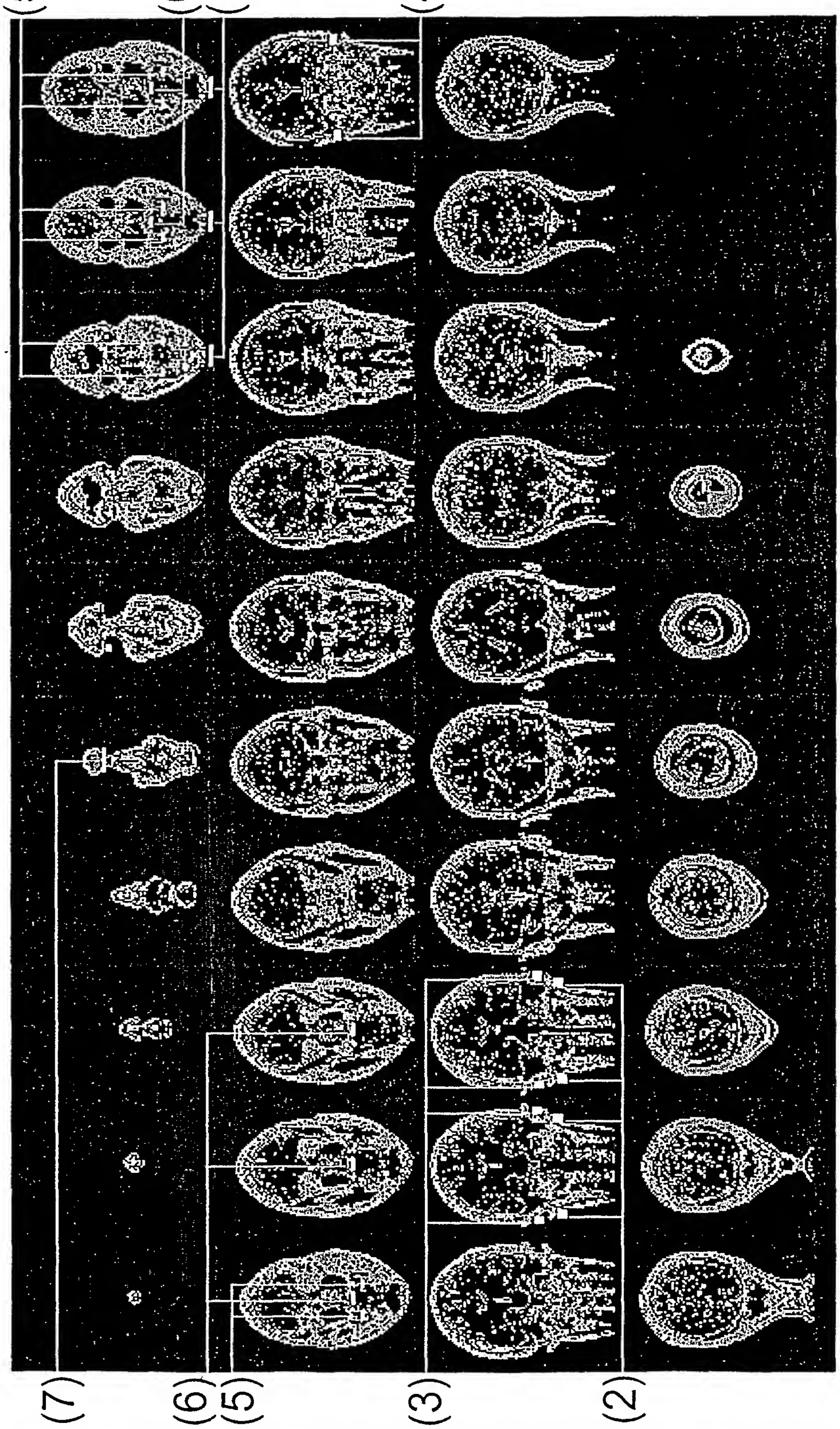

Fig. 9

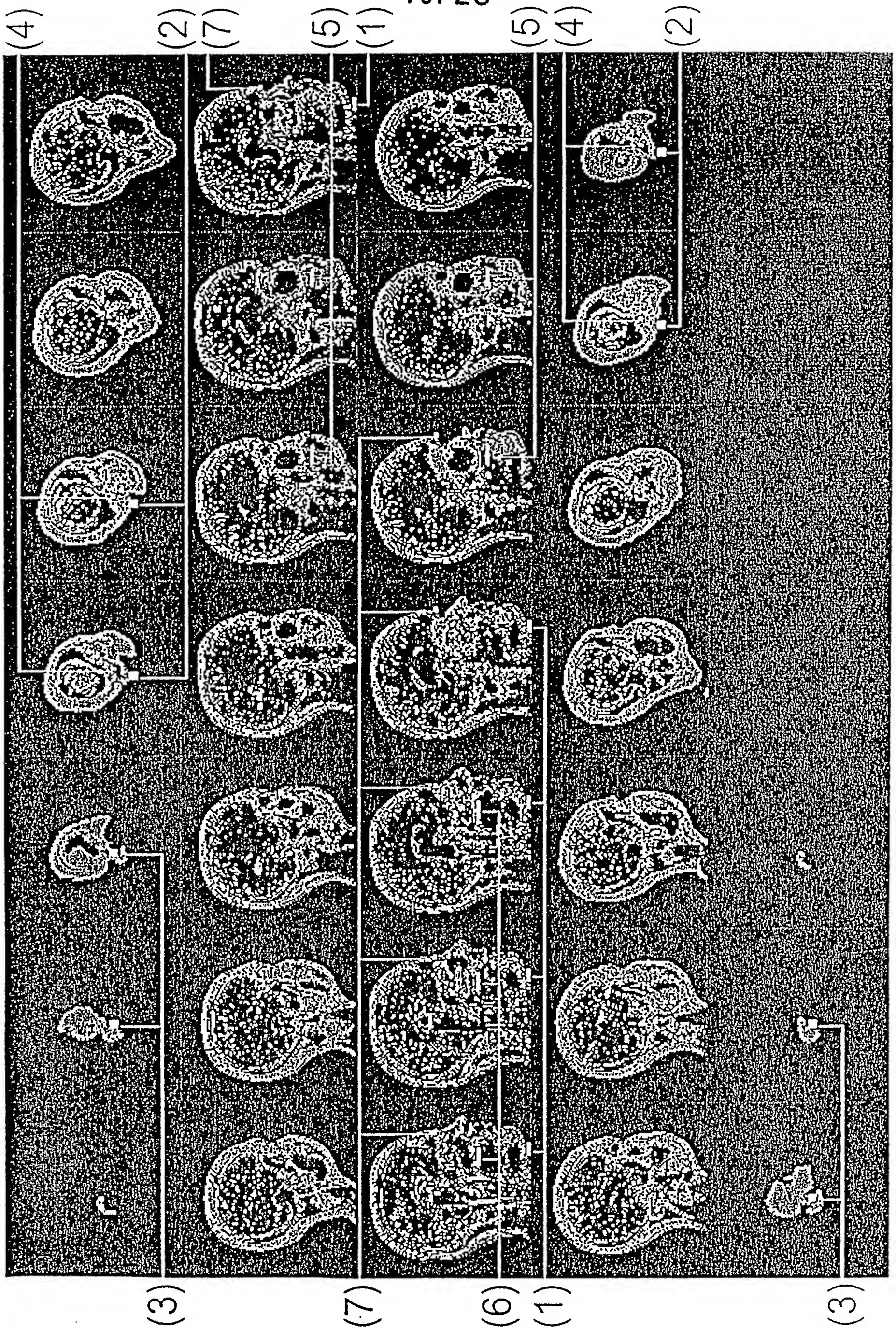

Fig. 10

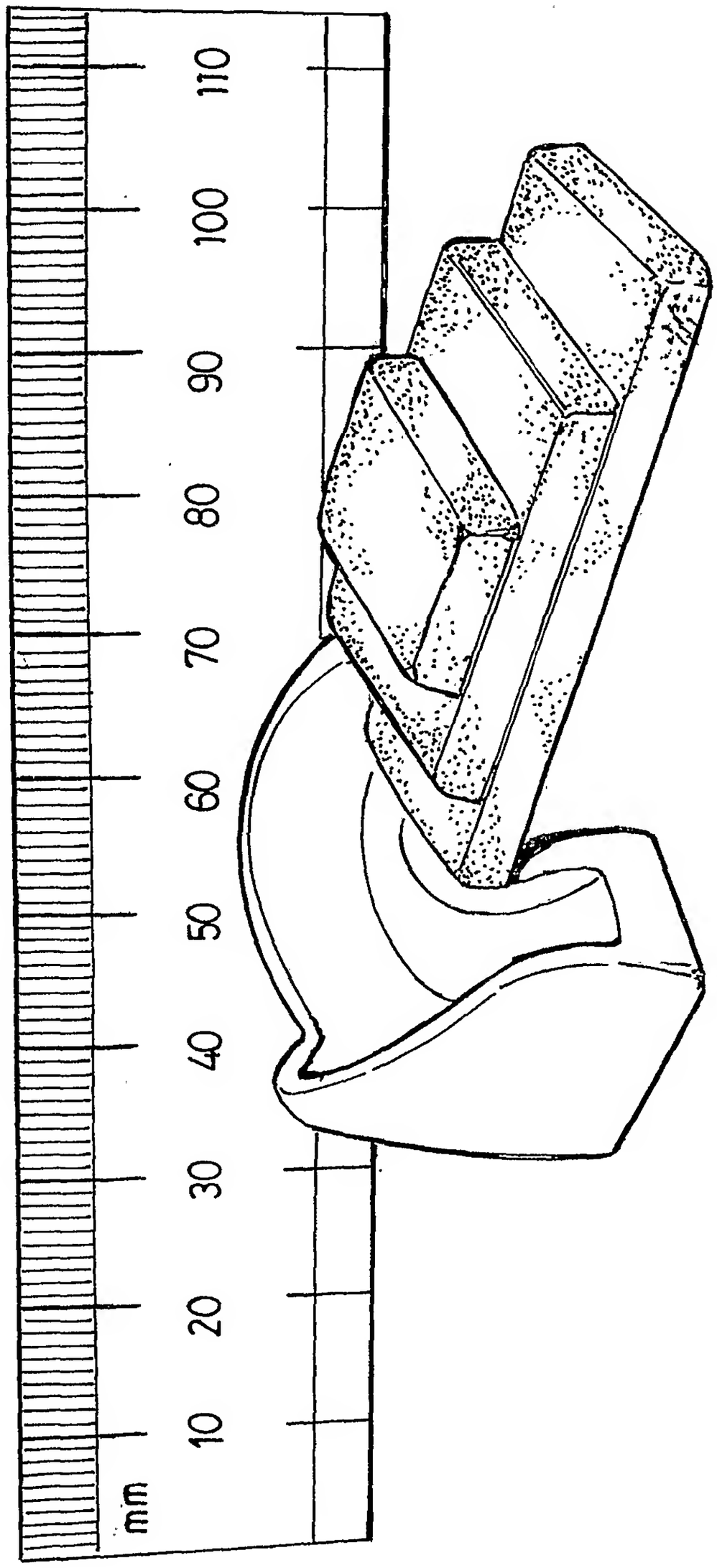

Fig. 11

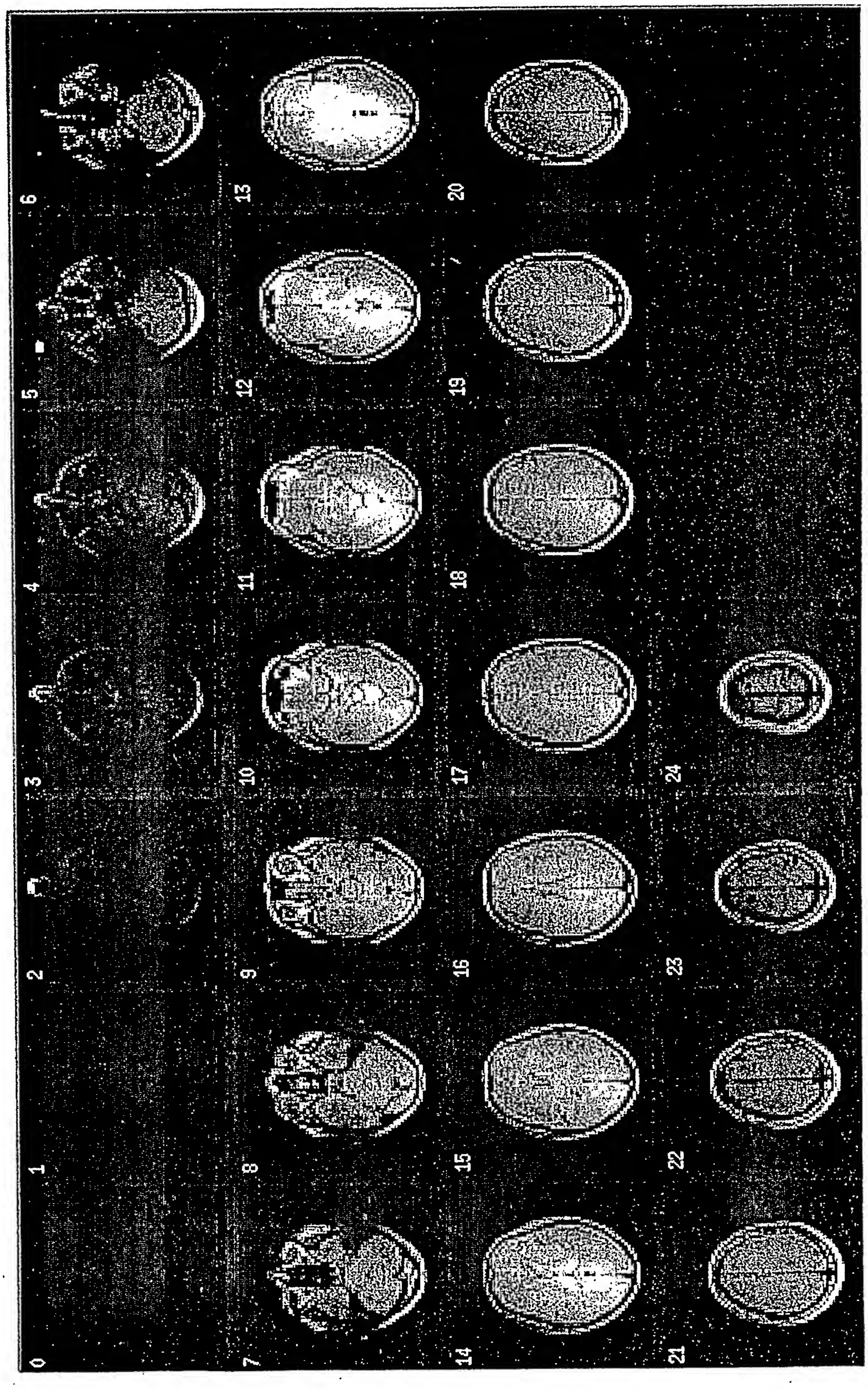

Fig. 12

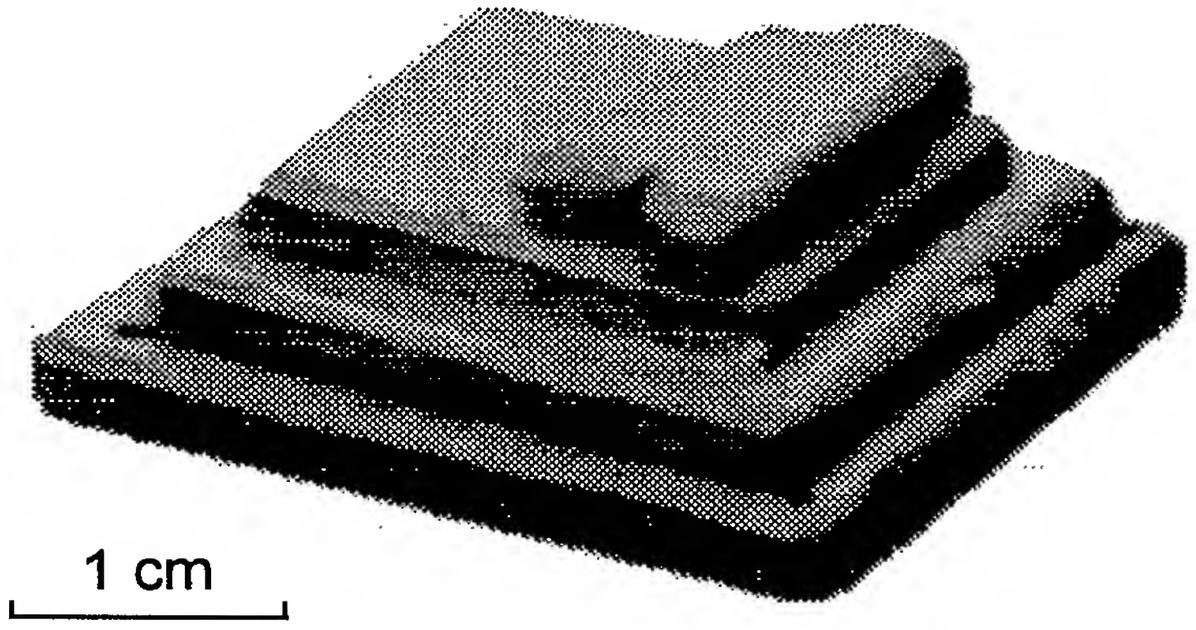

Fig. 13

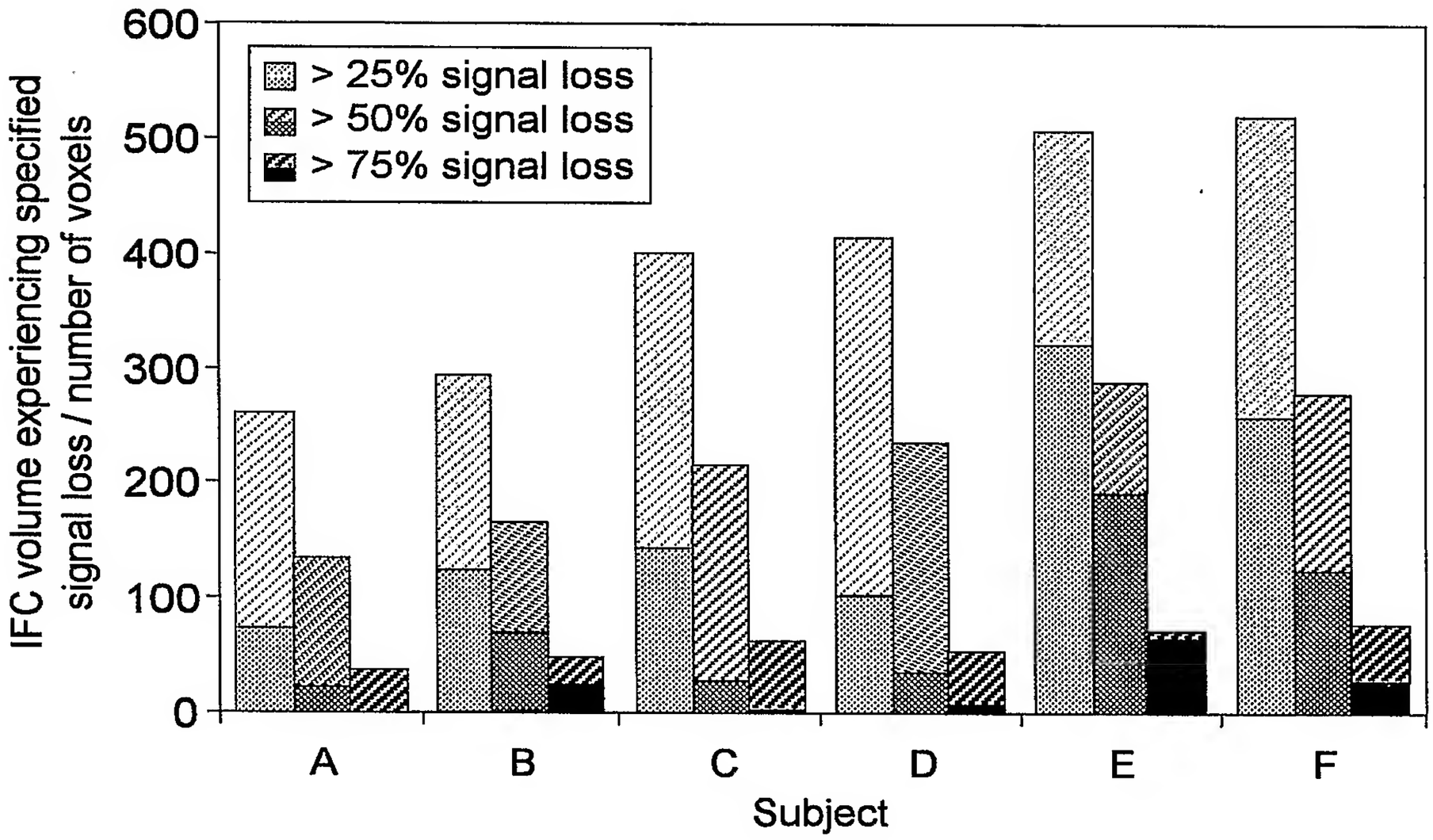
> 25% signal loss
> 50% signal loss
> 75% signal loss
IFC volume experiencing specified signal loss / number of voxels
600
500
400
300
200
100
0
A
B
C
D
E
F
Subject

Fig. 14

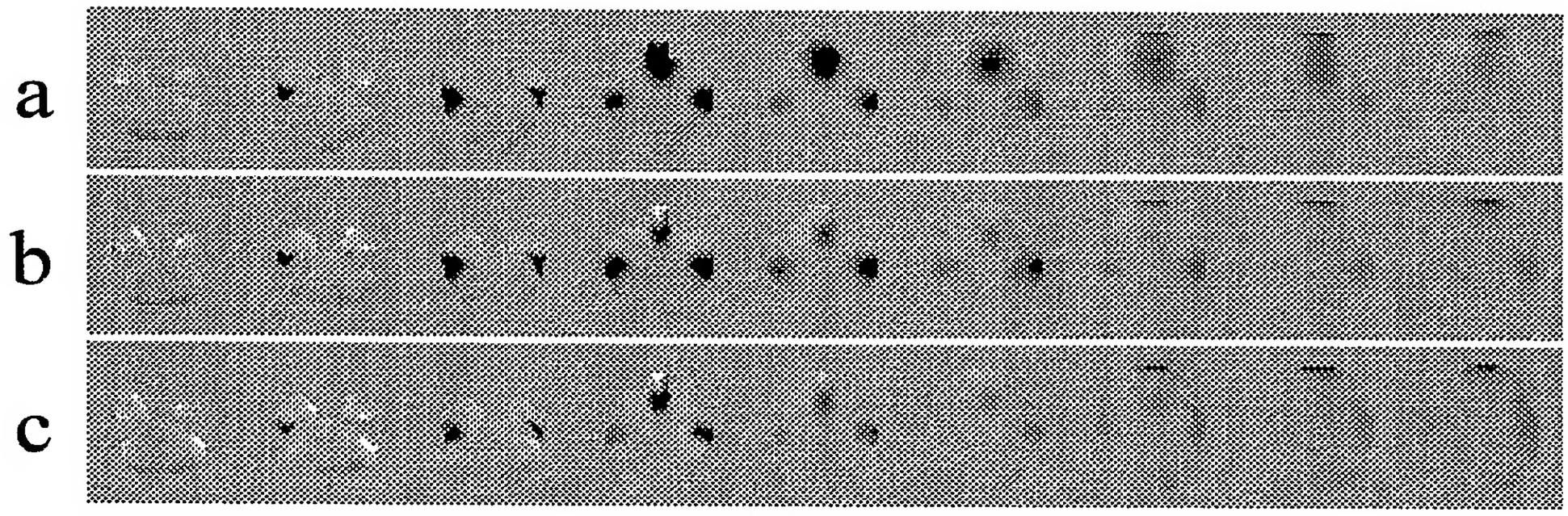

Fig. 15

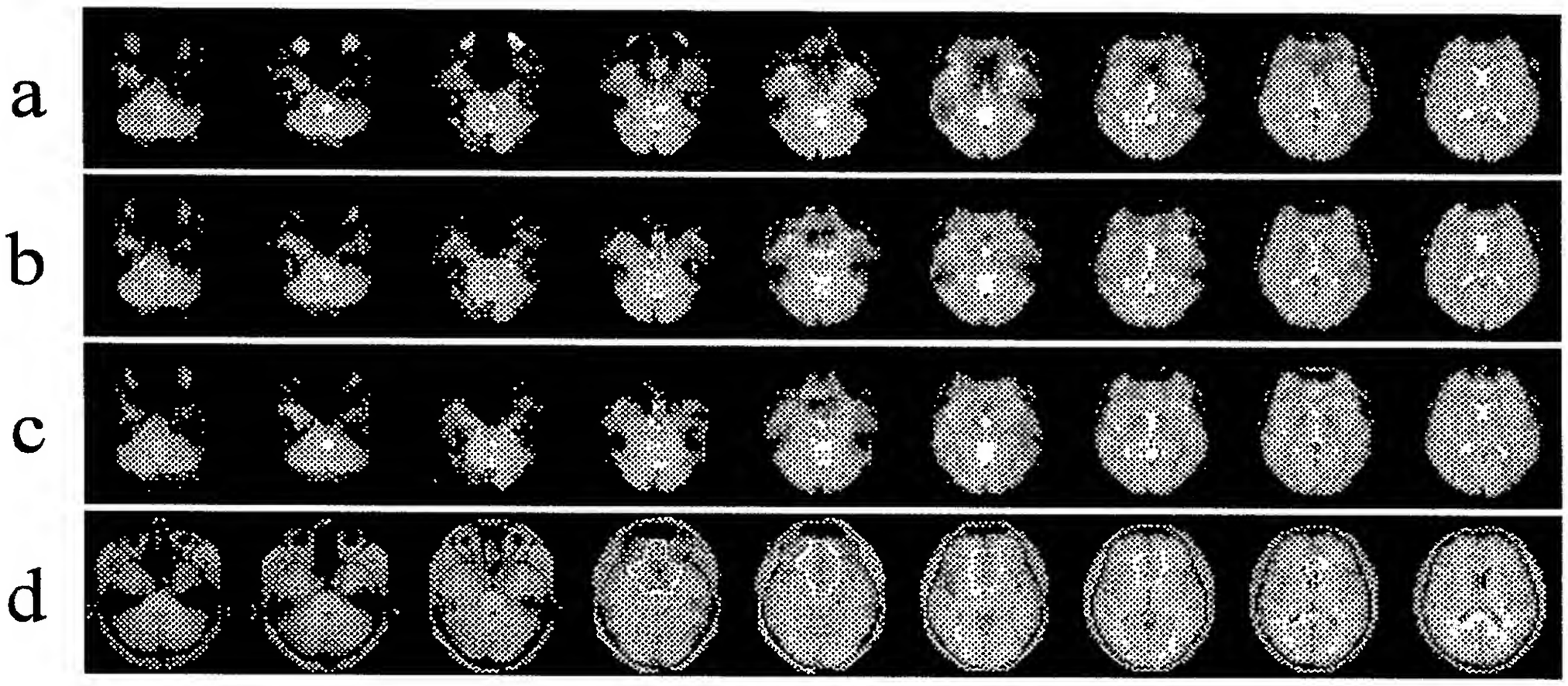

Fig. 16

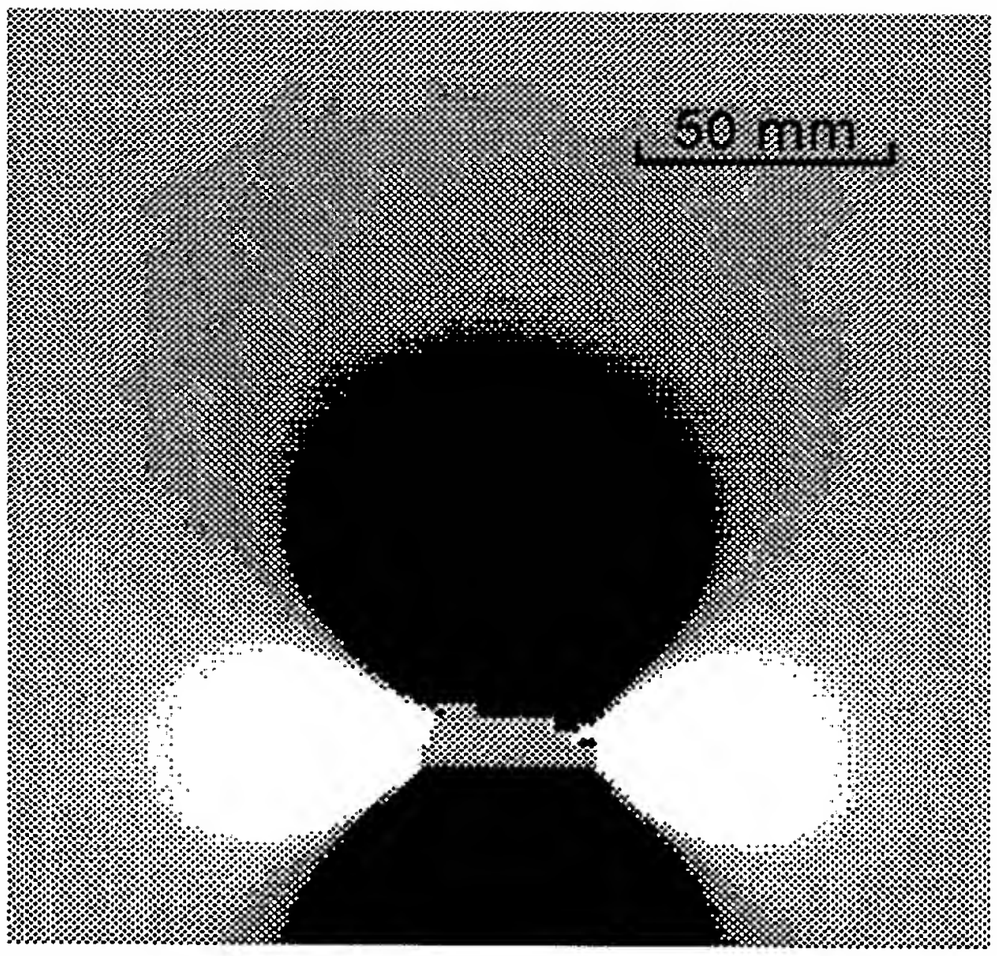

Fig. 17a

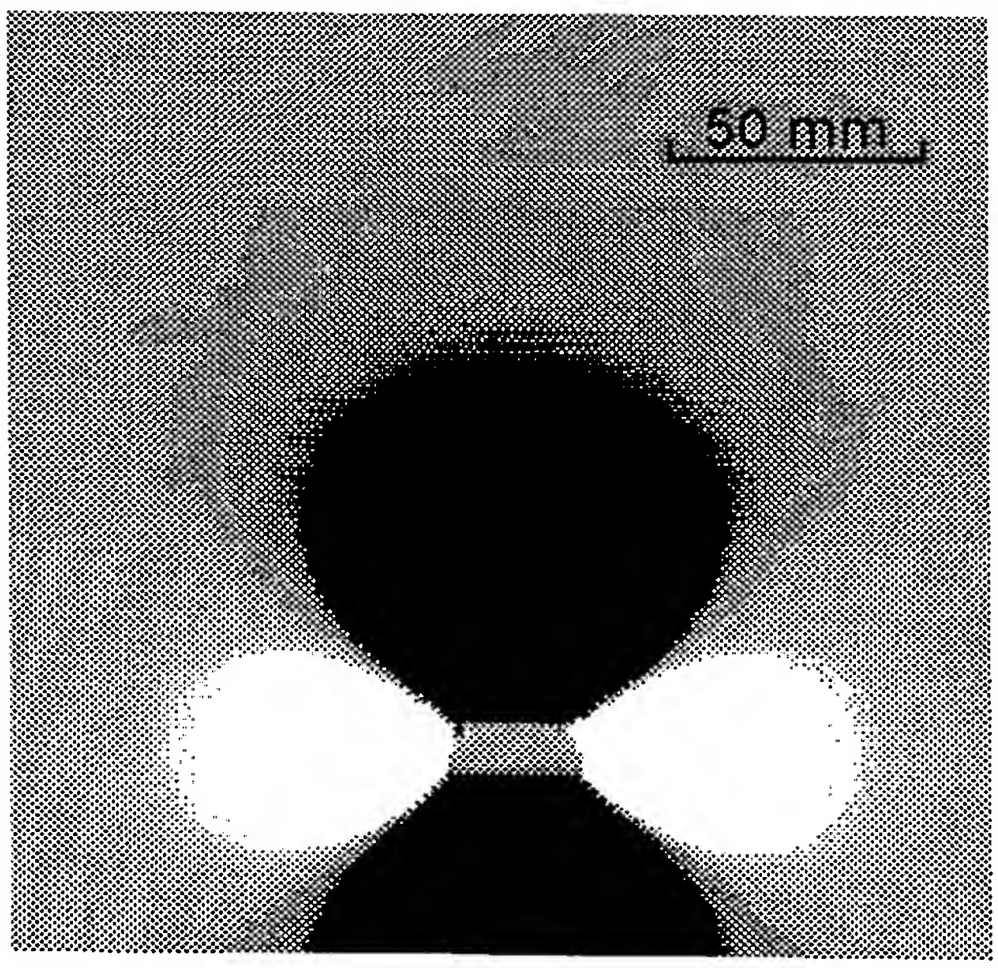

Fig. 17b

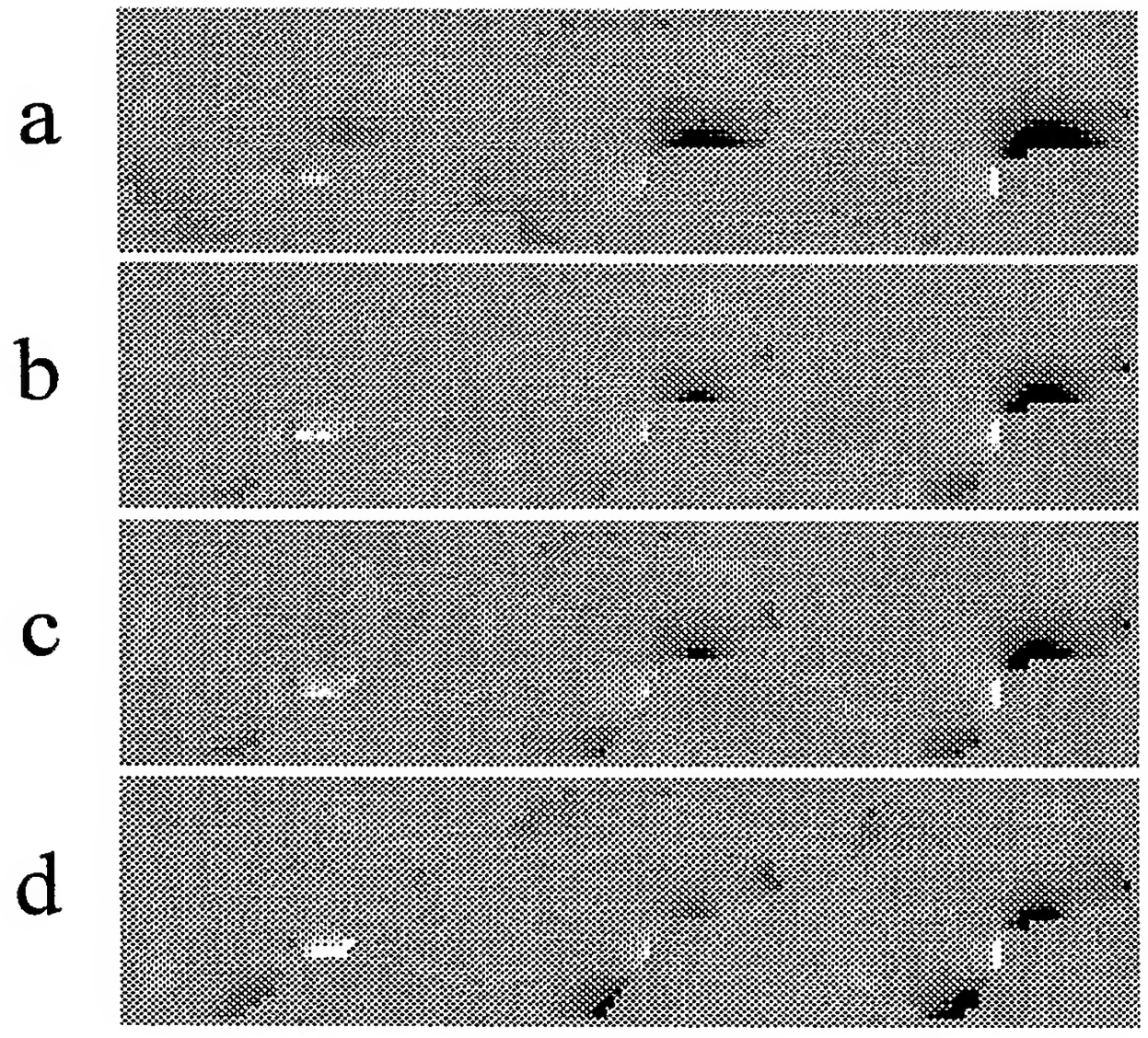

Fig.18

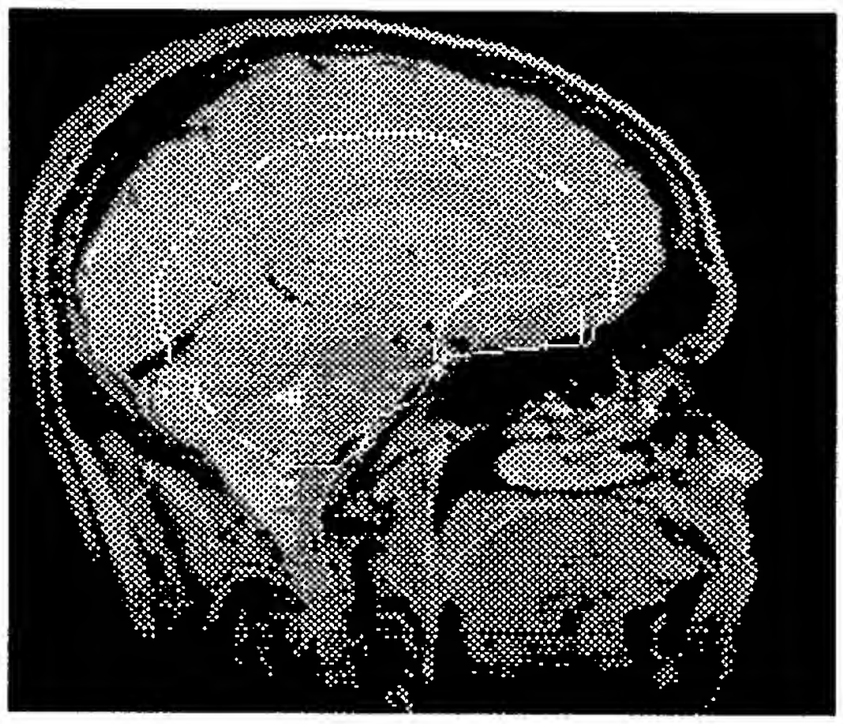

Fig.19a

Fig.19b

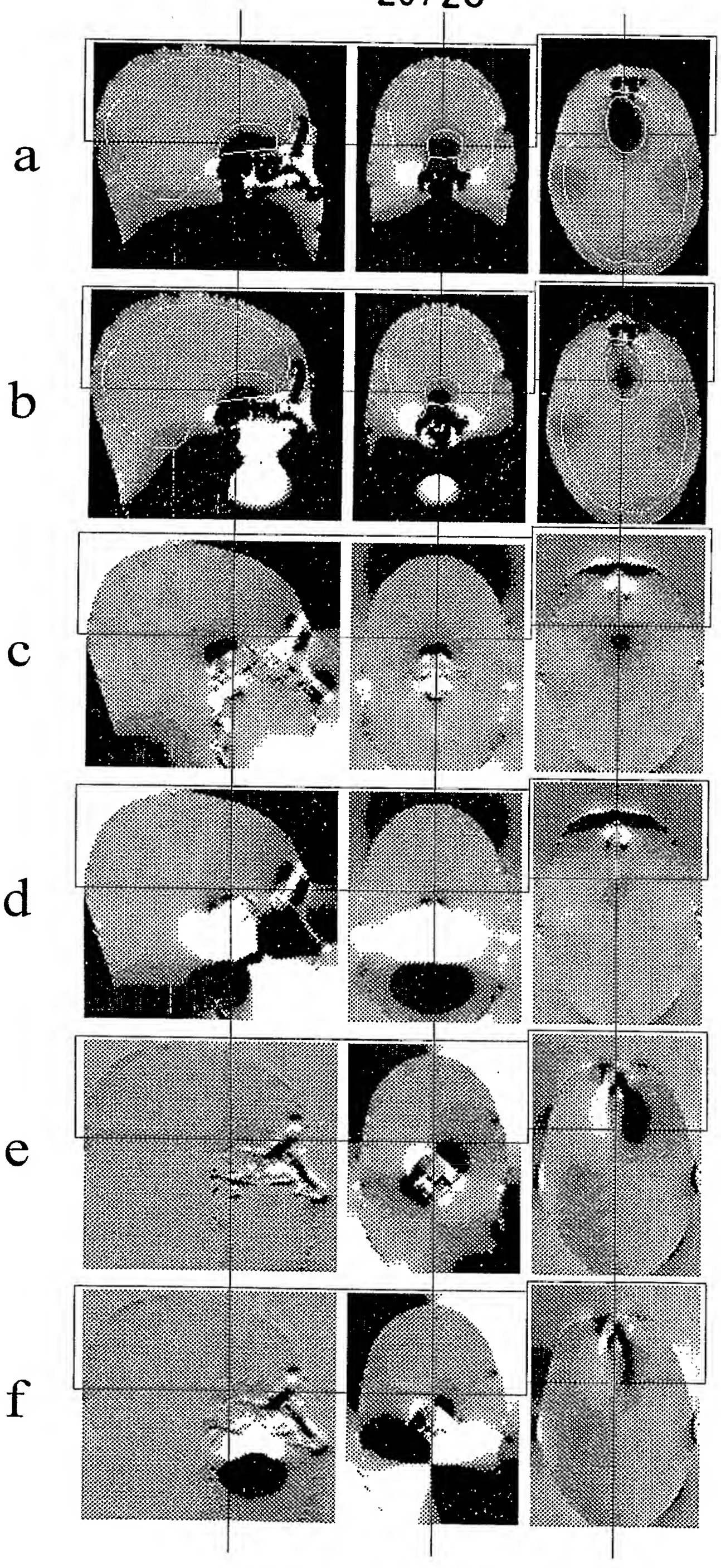

Fig. 20

Fig. 21a

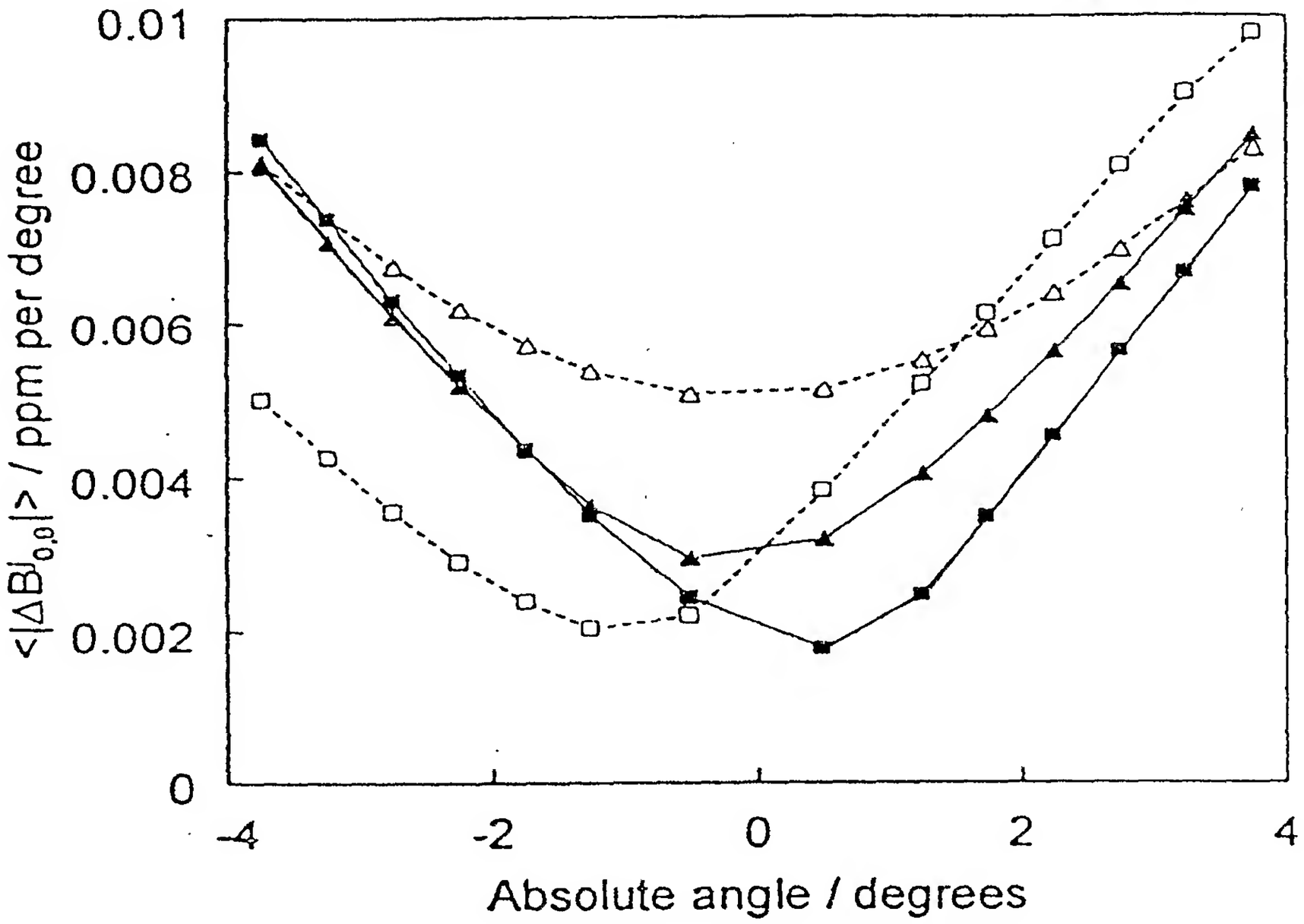

Fig. 21b

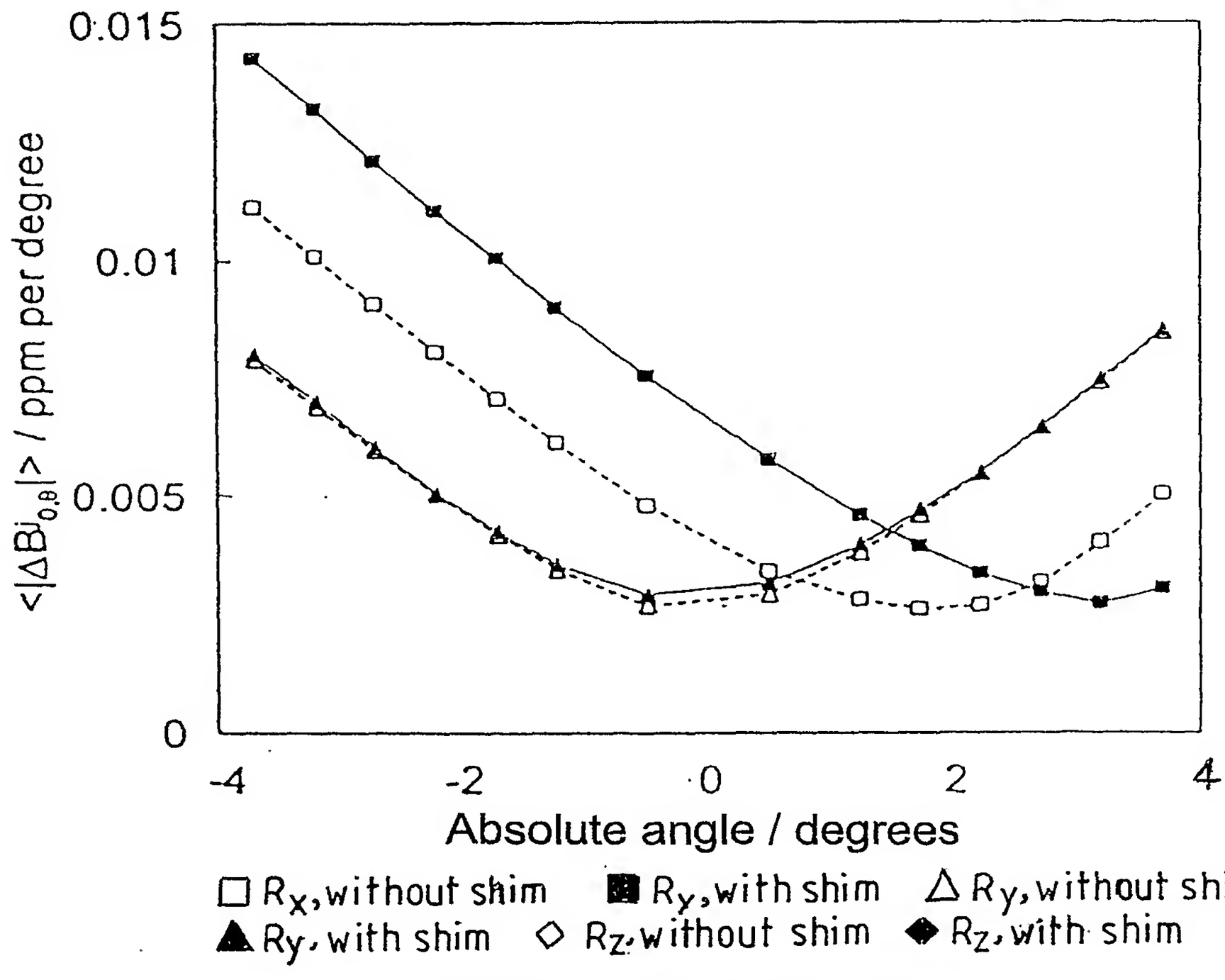

Fig. 21c

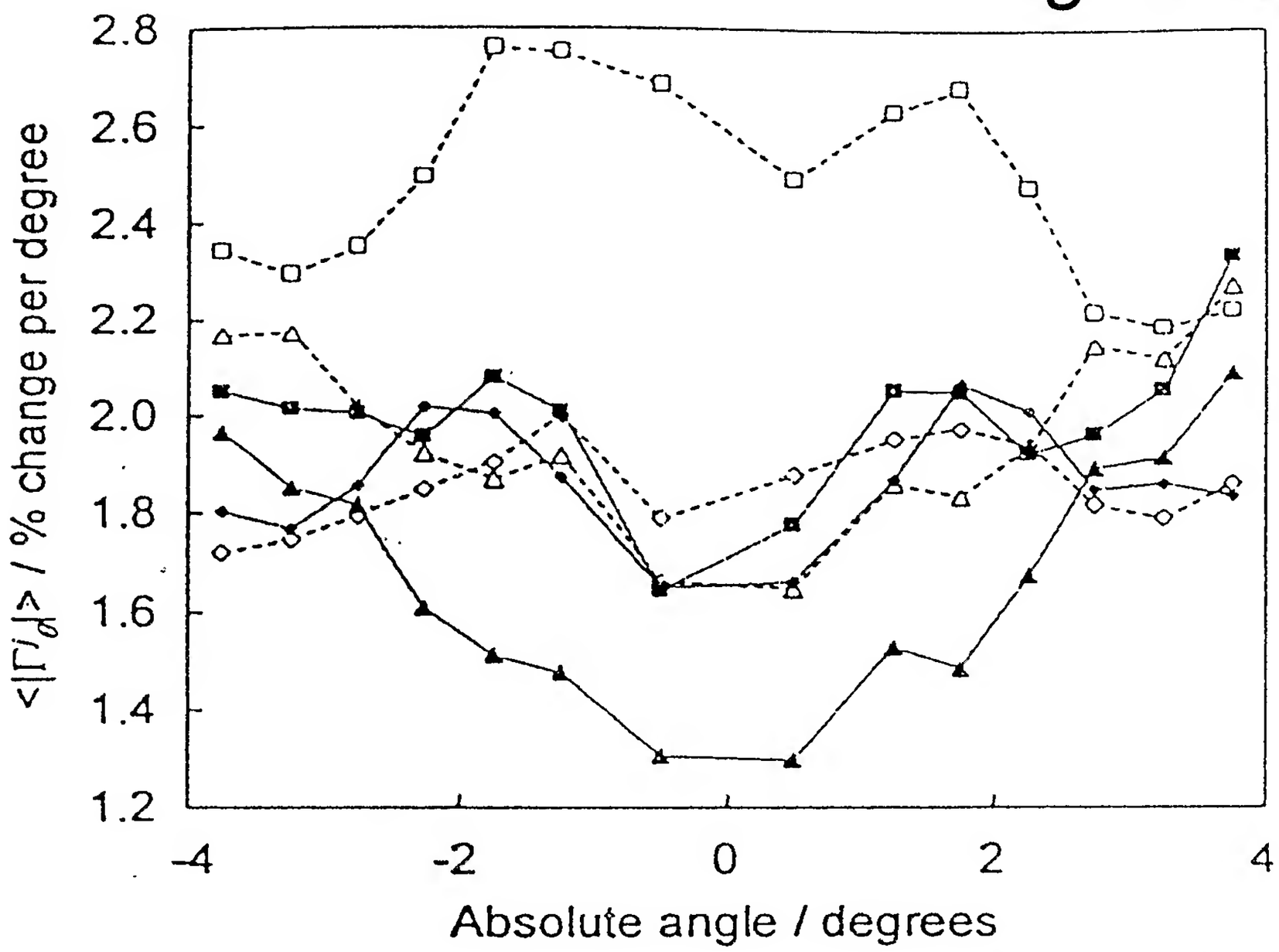

Fig. 21d

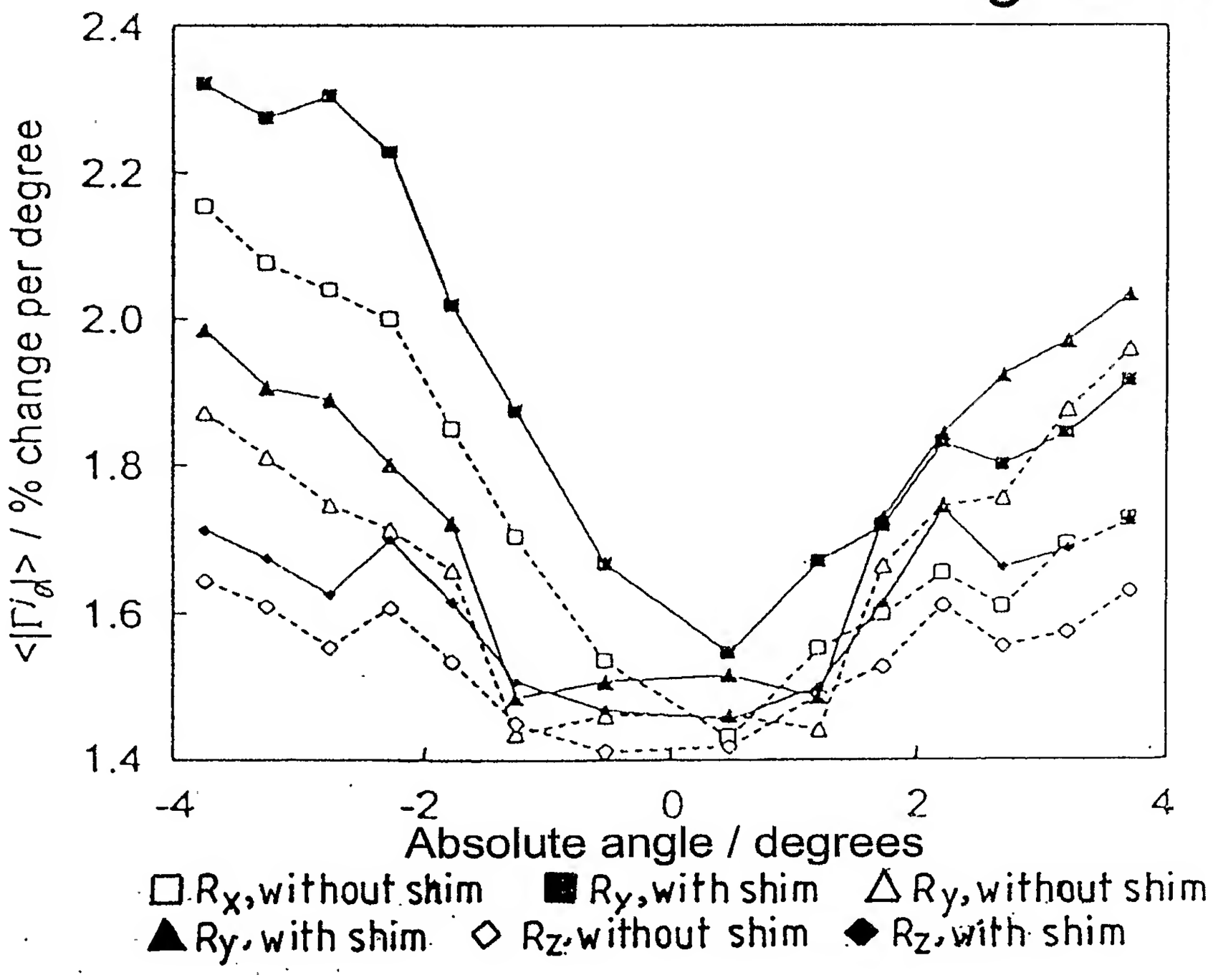

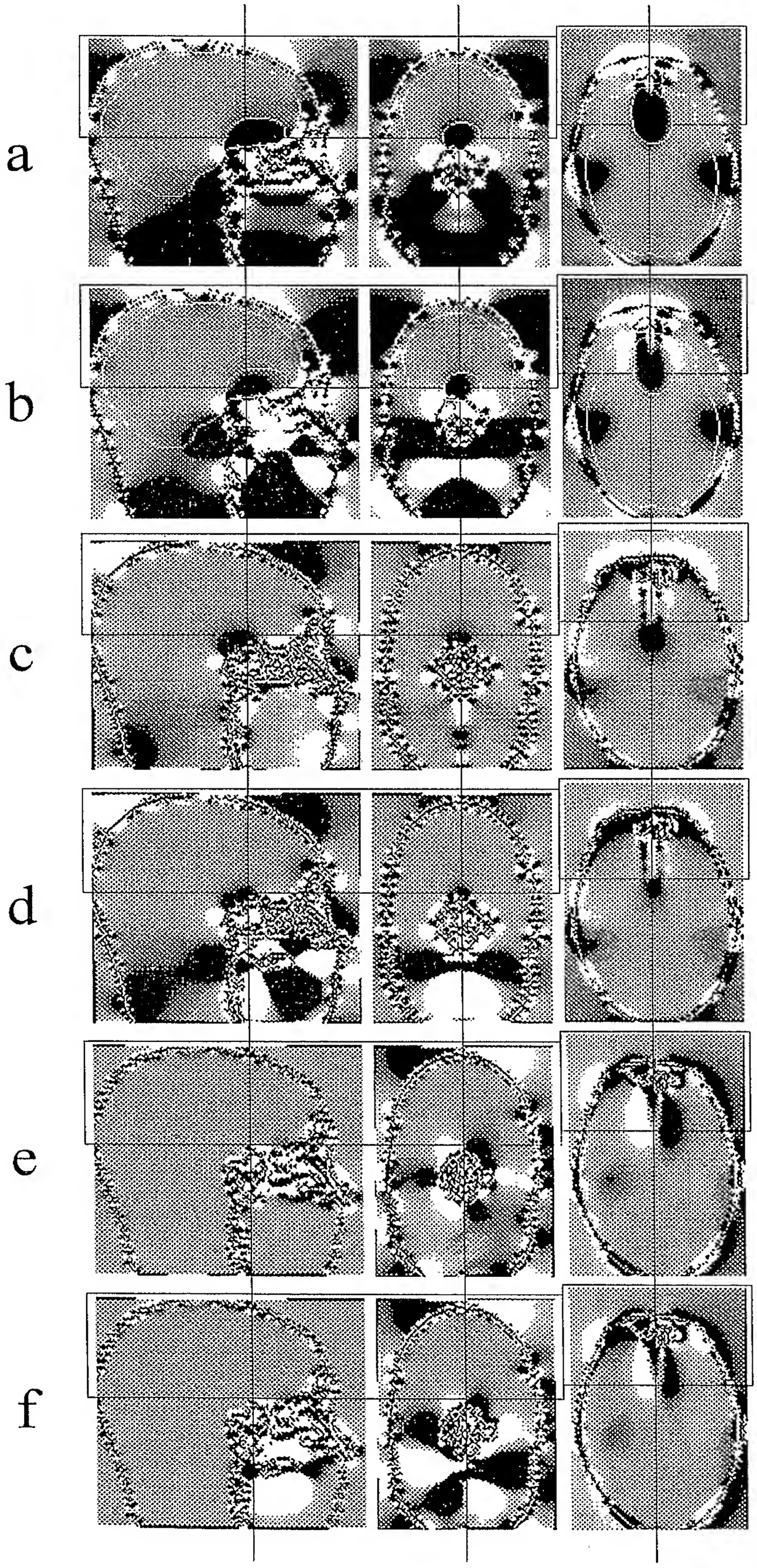

Fig. 22

Fig. 23a

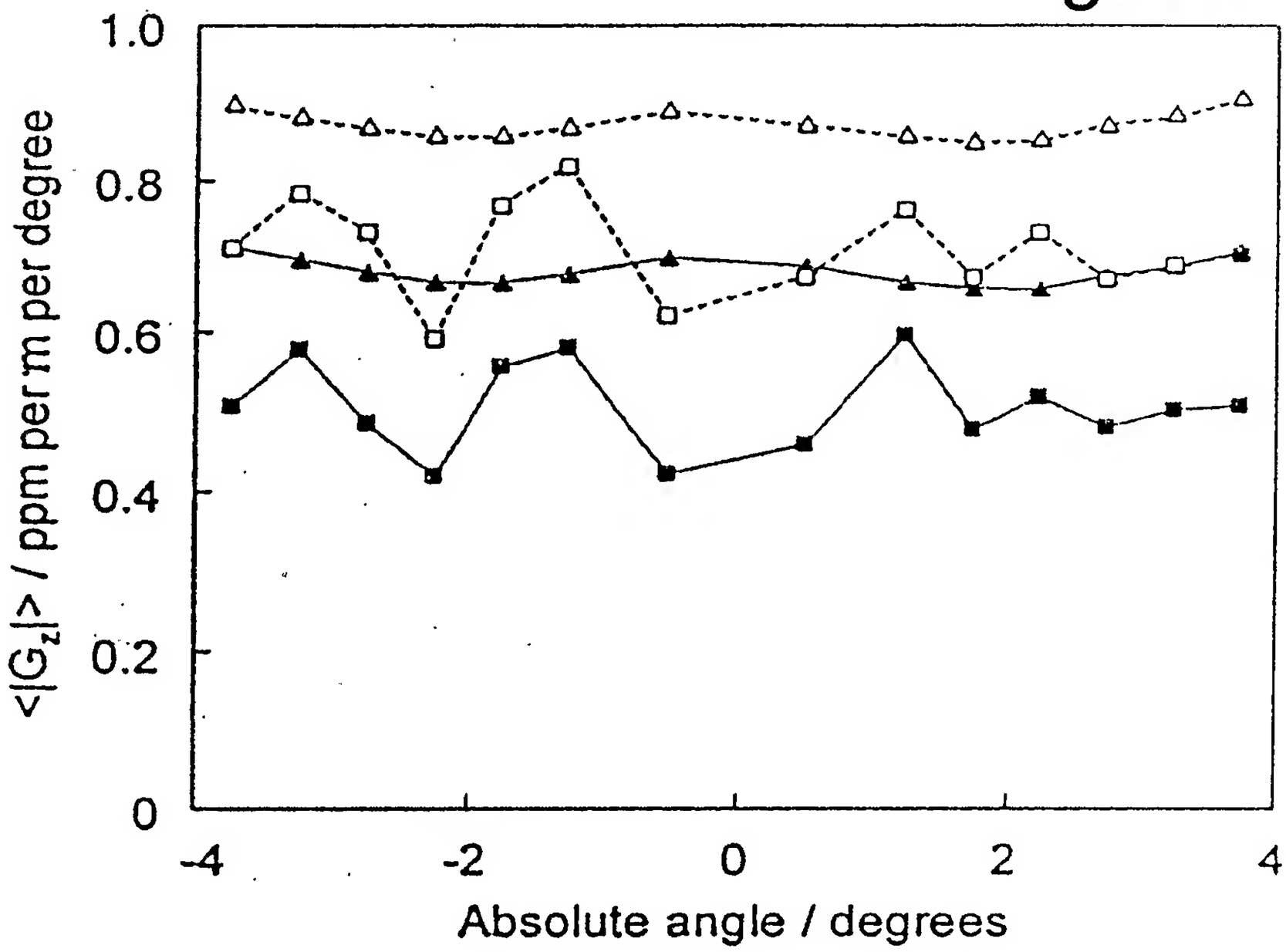

Fig. 23b

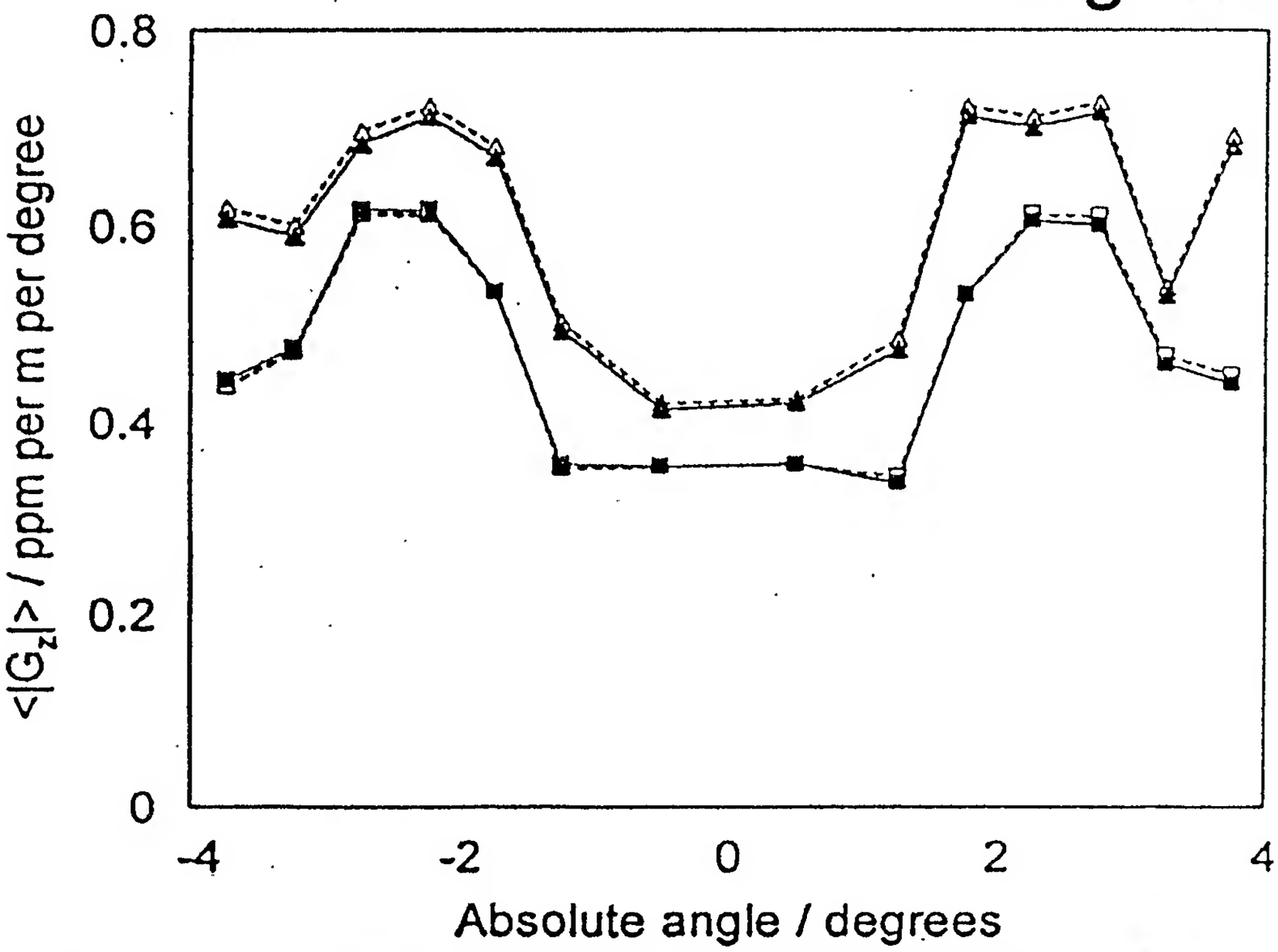

Fig. 23c

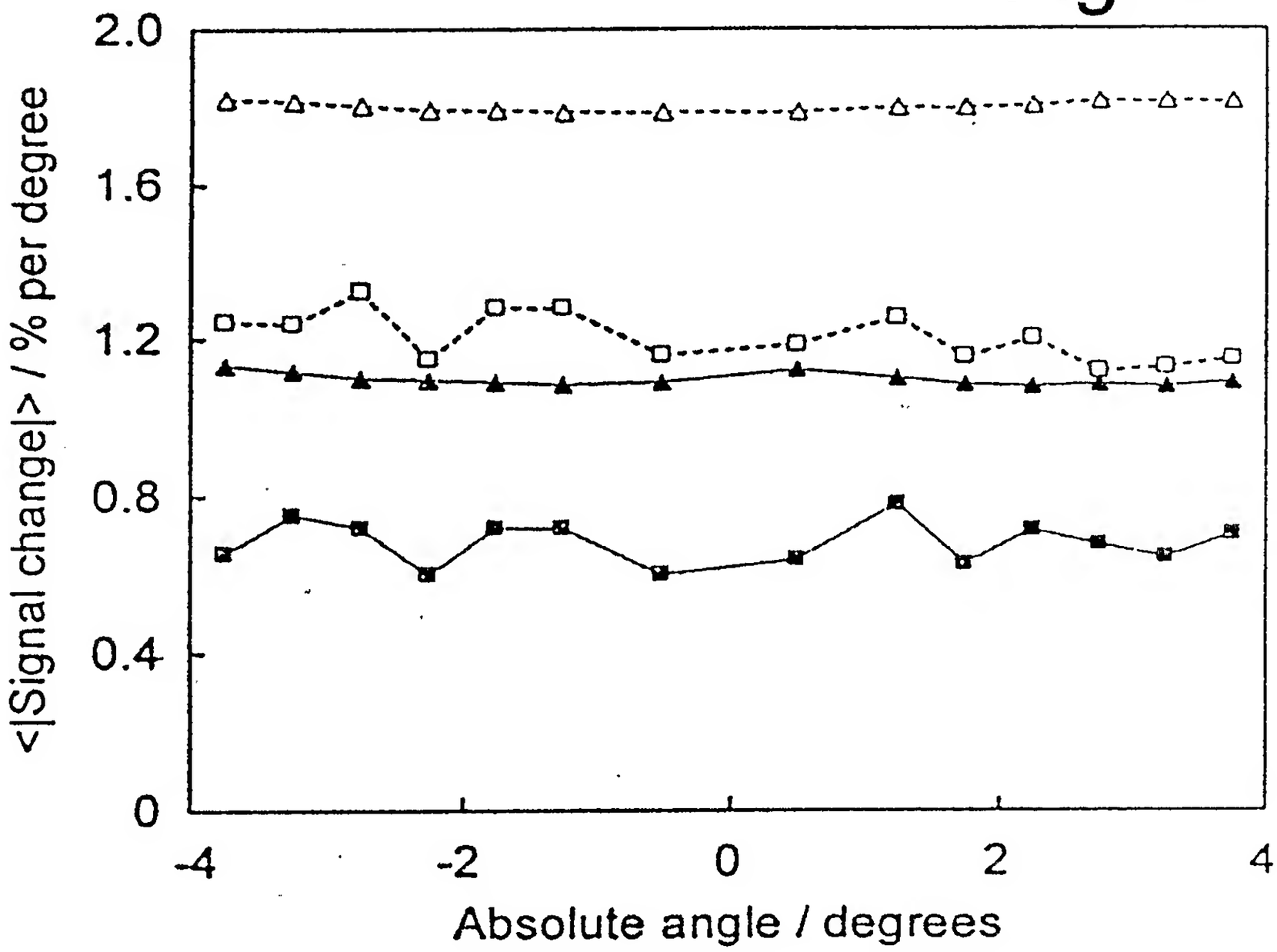

Fig. 23d

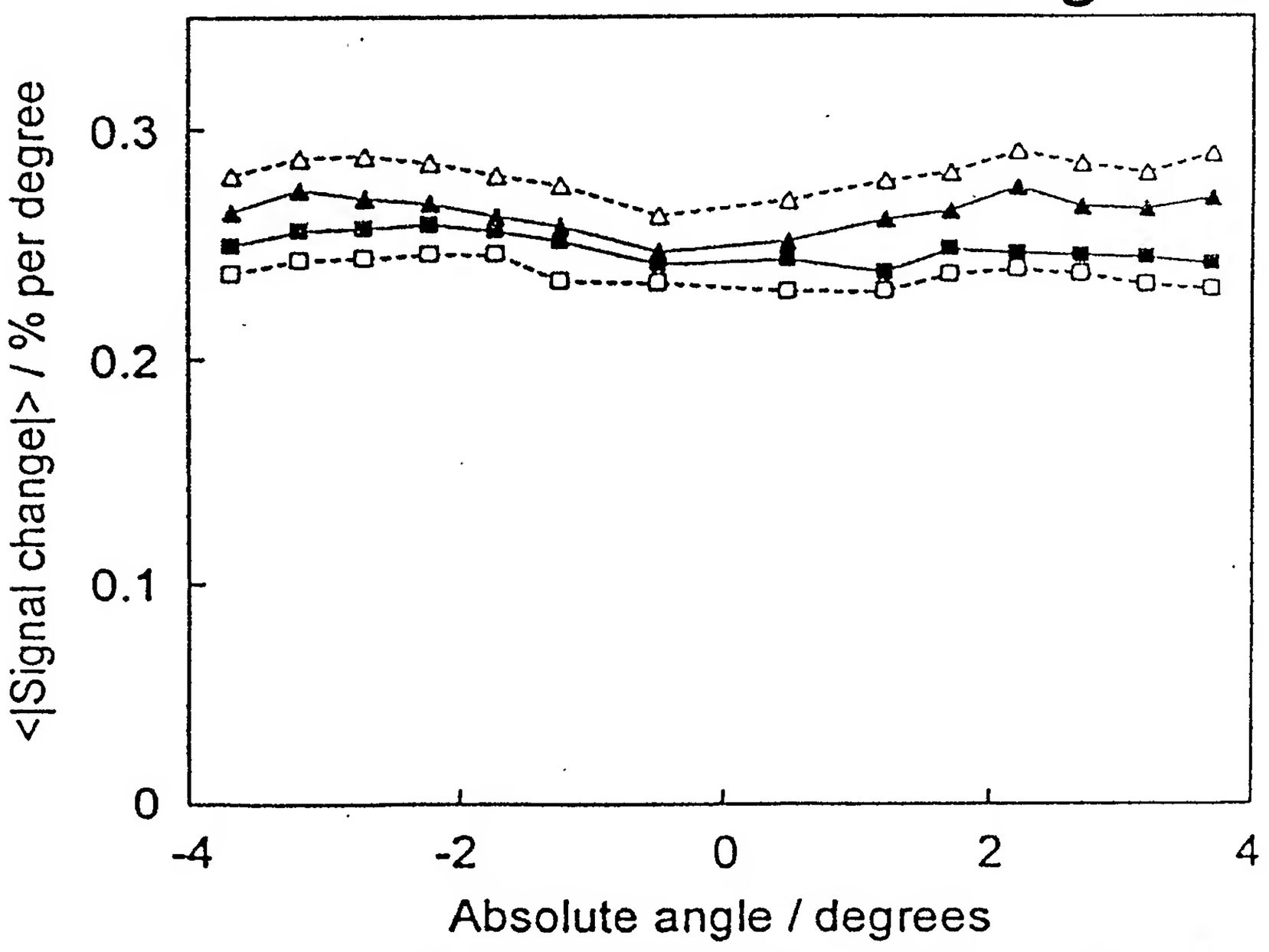

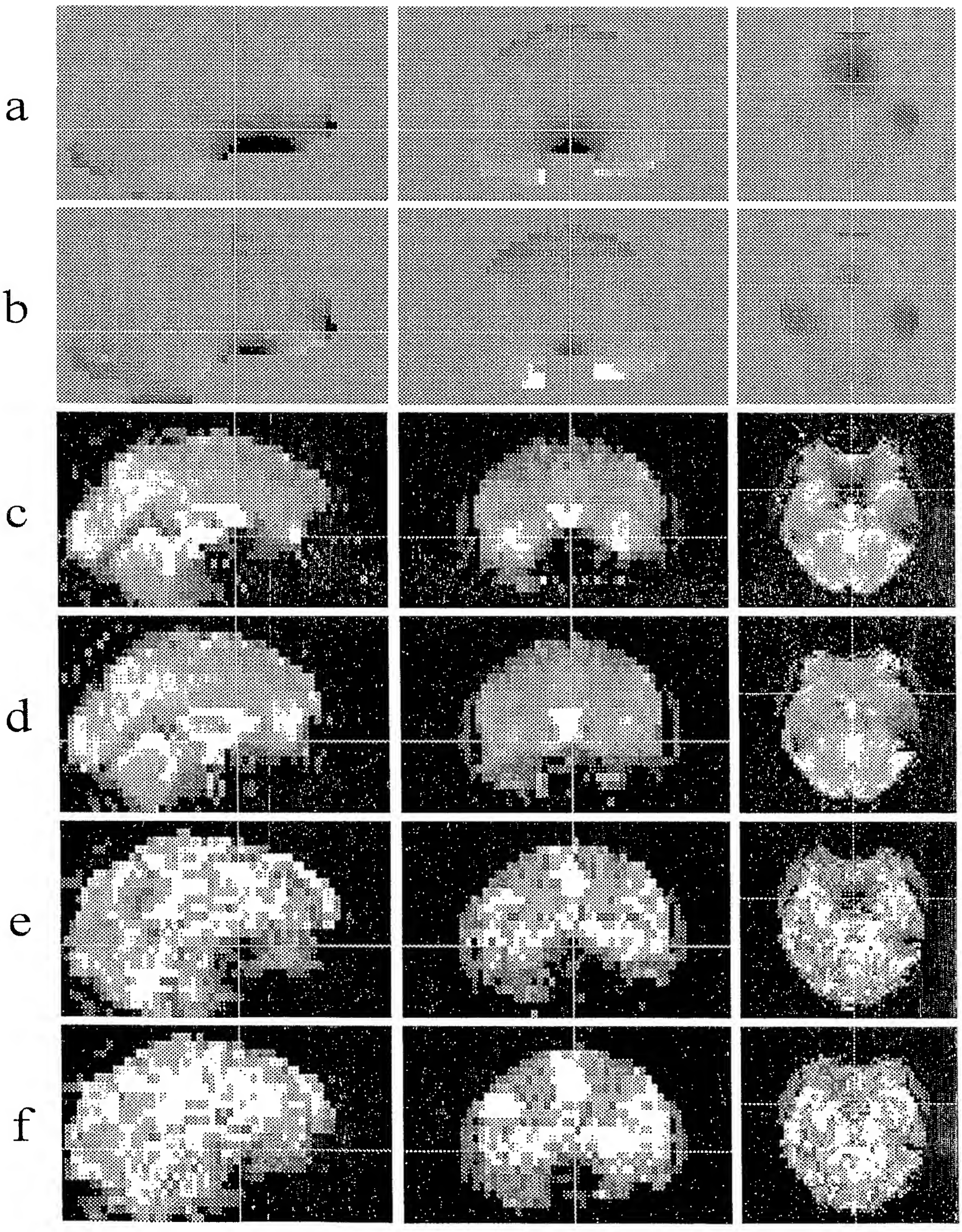

Fig. 24

INTERNATIONAL SEARCH REPORT

Intern al Application No
PCT/GB 03/00313

A. CLASSIFICATION OF SUBJECT MATTER
IPC 7 G01R33/387

According to International Patent Classification (IPC) or to both national classification and IPC

B. FIELDS SEARCHED

Minimum documentation searched (classification system followed by classification symbols)
IPC 7 G01R A61B

Documentation searched other than minimum documentation to the extent that such documents are included in the fields searched

Electronic data base consulted during the international search (name of data base and, where practical, search terms used)
EPO-Internal, MEDLINE, INSPEC, WPI Data, EMBASE, PAJ, COMPENDEX

C. DOCUMENTS CONSIDERED TO BE RELEVANT

Category °	Citation of document, with indication, where appropriate, of the relevant passages	Relevant to claim No.
X	US 5 173 661 A (KNUETTEL BERTOLD ET AL) 22 December 1992 (1992-12-22) column 1, line 19 -column 2, line 46 column 7, line 1 - line 12	1-5,7-9, 11,12,14
Y	---	6
Y	US 5 111 146 A (KUHN MICHAEL H) 5 May 1992 (1992-05-05) column 1, line 28 - line 40 column 2, line 32 -column 3, line 12	6
X	---	1,18-20
	US 5 339 033 A (EILENBERG STEVEN S ET AL) 16 August 1994 (1994-08-16) column 3, line 35 - line 50 column 8, line 43 - line 59	

	-/--	

[X] Further documents are listed in the continuation of box C.

[X] Patent family members are listed in annex.

° Special categories of cited documents :

"A" document defining the general state of the art which is not considered to be of particular relevance

"E" earlier document but published on or after the international filing date

"L" document which may throw doubts on priority claim(s) or which is cited to establish the publication date of another citation or other special reason (as specified)

"O" document referring to an oral disclosure, use, exhibition or other means

"P" document published prior to the international filing date but later than the priority date claimed

"T" later document published after the international filing date or priority date and not in conflict with the application but cited to understand the principle or theory underlying the invention

"X" document of particular relevance; the claimed invention cannot be considered novel or cannot be considered to involve an inventive step when the document is taken alone

"Y" document of particular relevance; the claimed invention cannot be considered to involve an inventive step when the document is combined with one or more other such documents, such combination being obvious to a person skilled in the art.

"&" document member of the same patent family

Date of the actual completion of the international search	Date of mailing of the international search report
10 April 2003	29/04/2003

Name and mailing address of the ISA	Authorized officer
European Patent Office, P.B. 5818 Patentlaan 2 NL – 2280 HV Rijswijk Tel. (+31–70) 340–2040, Tx. 31 651 epo nl, Fax: (+31–70) 340–3016	Skalla, J

INTERNATIONAL SEARCH REPORT

Interr al Application No
PCT/GB 03/00313

C.(Continuation) DOCUMENTS CONSIDERED TO BE RELEVANT

Category °	Citation of document, with indication,where appropriate, of the relevant passages	Relevant to claim No.
X	FR 1 444 781 A (SCOTT PAPER CO) 8 July 1966 (1966-07-08) page 4, left-hand column, paragraph 2 ---	18,19
P,X	WILSON J L ET AL: "OPTIMIZATION OF STATIC FIELD HOMOGENEITY IN HUMAN BRAIN USING DIAMAGNETIC PASSIVE SHIMS" MAGNETIC RESONANCE IN MEDICINE, ACADEMIC PRESS, DULUTH, MN, US, vol. 48, no. 5, November 2002 (2002-11), pages 906-914, XP001130533 ISSN: 0740-3194 * the entire document * ---	1-21
A	US 6 294 972 B1 (JESMANOWICZ ANDRZEJ ET AL) 25 September 2001 (2001-09-25) column 1, line 51 -column 3, line 13 ---	1-17
A	JESMANOWICZ A. ET AL: "Local Ferroshims Using Office Copier Toner" PROCEEDINGS OF THE INTERNATIONAL SOCIETY FOR MAGNETIC RESONANCE IN MEDICINE, 9TH SCIENTIFIC MEETING AND EXHIBITION, vol. 1, 21 April 2001 (2001-04-21), page 617 XP002237881 Glasgow, Scotland abstract -----	1-17

INTERNATIONAL SEARCH REPORT

Information on patent family members

Inter nal Application No
PCT/GB 03/00313

Patent document cited in search report	Publication date	Patent family member(s)	Publication date
US 5173661 A	22-12-1992	DE 3937150 A1	23-05-1991
		GB 2237883 A ,B	15-05-1991
US 5111146 A	05-05-1992	DE 3917619 A1	06-12-1990
		EP 0400733 A2	05-12-1990
		JP 3162832 A	12-07-1991
US 5339033 A	16-08-1994	AT 180895 T	15-06-1999
		AU 673191 B2	31-10-1996
		AU 4803793 A	15-03-1994
		CA 2142302 A1	03-03-1994
		DE 69325184 D1	08-07-1999
		DE 69325184 T2	09-03-2000
		DK 714518 T3	15-11-1999
		EP 0714518 A1	05-06-1996
		ES 2131587 T3	01-08-1999
		GR 3030743 T3	30-11-1999
		JP 8500267 T	16-01-1996
		WO 9404946 A1	03-03-1994
		US 5414358 A	09-05-1995
FR 1444781 A	08-07-1966	DE 1504888 A1	28-01-1971
		GB 1112896 A	08-05-1968
		MY 16769 A	31-12-1969
US 6294972 B1	25-09-2001	NONE	